Dissecting the role of Adnp in neurogenesis using the mouse retina as a model system

SUMA MEDISETTI

Thesis submitted to the University of Ottawa in partial
Fulfillment of the requirements for the Master's degree in Neuroscience

Department of Neuroscience, Faculty of Medicine
University of Ottawa

GRAPHICAL ABSTRACT

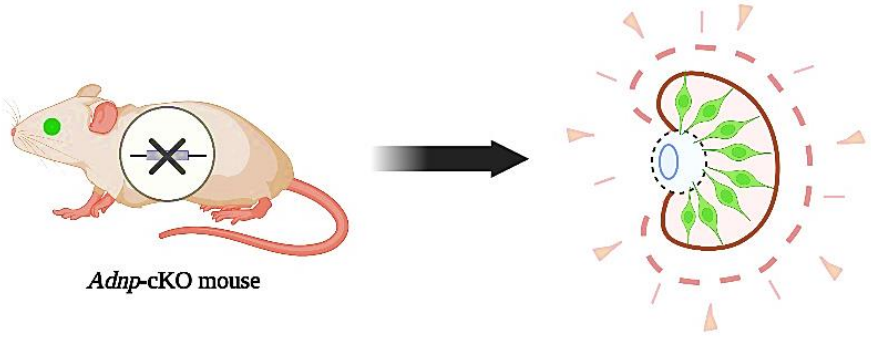

Created with BioRender.com

ABSTRACT

The *ADNP* (Activity dependent neuroprotective protein) gene encodes a transcription factor that is essential for embryonic development and brain formation. Mutations within this gene cause a neurodevelopmental disorder known as Helsmoortel-Van Der Aa syndrome. *ADNP* is one of the most commonly mutated single genes associated with autism spectrum disorder. However, its role in neurodevelopment is unclear. Our goal in this study is to dissect the role of *Adnp* in neurogenesis using the mouse retina as a tractable model system. We hypothesized that *Adnp* might have a crucial role in retinal neurogenesis. We found that Adnp was consistently expressed in all progenitor cells throughout retinal development. Interestingly, Adnp expression was relatively high in differentiated cells and persisted in the adult retina. Adnp was found to regulate retinal size, possibly by controlling cell survival during retinal development. In the retina, Adnp was found to interact with the Chd4 chromodomain helicase protein and might therefore be involved in chromatin remodelling. On the other hand, it also interacted with Pogz – a zinc finger protein associated with heterochromatin and might have a specific role in neural gene regulation. Altogether, these findings indicate that Adnp plays a crucial role in retinal neurogenesis and identify possible neurodevelopmental mechanisms that might depend on Adnp.

ACKNOWLEDGEMENTS

First and foremost, I must say that I am extremely fortunate to work on this exciting project and I very grateful to my supervisor Dr. Pierre Mattar for his utmost support and guidance. I am very thankful for providing the information needed while I take course from India and helping me to settle in the lab after reaching here. Thanks for the scheduling study meetings and helping me to prepare to transfer exam. His continuous guidance and feedback had helped me to stay on track and work towards the priorities. I could not have imagined having a better advisor and mentor.

I would like to thank my thesis advisory committee members, Dr. Catherine Tsilfidis and Dr. Baptiste Lacoste for their insightful remarks and suggestions.

I thank Samuel Clémot-Dupont for all the help with mouse work and helping me with genotyping when needed. Thanks to Sujay Shah for sharing your knowledge and particular handling retina and confocal microscopy. I am grateful to have friendly and cheerful lab members- Sarah Larrigan, Alex Fernandes and Ivana Nad for their immense support which really means a lot to me. The affection and care I received from all of them will be in my heart forever.

Thanks to the university for allowing me between master program as well as departments particularly with pandemic uncertainty. As an international student, I am intrigued by the academic curriculum and courses that help me expand my knowledge drastically. Moreover, seminars and research day conferences that helped me realise my strengths and made me better at time management and engaging communication.

Last but not least I owe immense gratitude to my parents, for unwavering support and love.

TABLE OF CONTENTS

LIST OF ABBREVIATIONS

LIST OF FIGURES

LIST OF TABLES

CHAPTER 1 INTRODUCTION

Neurogenesis is the process in which neural progenitors proliferate and produce different types of neurons. During embryonic development, it must be tightly controlled to ensure the proper functioning of the nervous system[1]. Despite decades of research on molecular mechanisms that regulate neurogenesis, it still remains incompletely understood. Moreover, with the increasing prevalence of neurodevelopmental disabilities, a deeper understanding of the factors that regulate neurogenesis and cause abnormalities in brain development has become more important. The retina is well known as a window to the brain and has been extensively studied for understanding the key concepts of neurogenesis over the years.

1.1 Brief introduction to eye and retina development

Murine eye development begins with formation of the optic sulcus , an outward pouch from the anterior neural plate, beginning around embryonic stage E8.0-8.5[2,3]. At this stage, the neuroepithelial cells express several eye field transcription factors (EFTFs), including Pax6, Rax, Six3, Lhx2, Vsx2, and Otx2, which act as positive regulators for retinal progenitor identity[4–6]. Mutations/knockdown of expression of such genes results in severe developmental defects, such as microphthalmia, anophthalmia and coloboma (optic fissure closure defects)[7,8]. As development proceeds, invagination forms the optic pit and its interactions with the overlying surface ectoderm lead to induction of the non-neural tissues of the eye: the lens and cornea (Figure 1.1). The concomitant invagination of the optic vesicle results in the formation of an optic cup (E10.5-11.0). The ciliary body, iris and pupillary muscles are derived from the anterior portion of the optic cup[9]. The Posterior portion of the optic cup is sub-divided into the retinal pigment epithelium (RPE),

neural retina and optic stalk (Figure 1.1). The neural retina contains retinal progenitor cells (RPCs) which further differentiate into seven basic cell types (six neuronal and one glial).

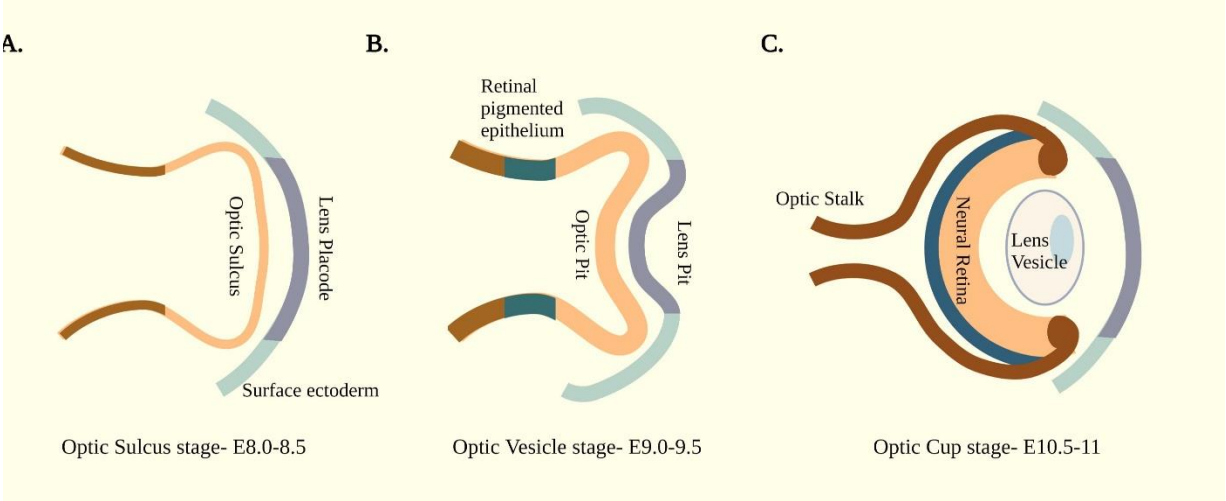

Figure 1.1 Schematic representation of mouse early eye morphogenesis

A) Optic Sulcus stage- Formation of optic sulcus from neuroepithelial cells and thickening of lens placode. B) Optic Vesicle stage- Invagination begins forming optic pit and interactions with the surface ectoderm form the lens pit. C) Optic Cup stage- Complete folding of the optic vesicle results in an early optic cup, where the retinal pigmented epithelium (blue) completely surrounds the neural retina (orange). The optic stalk develops from the undifferentiated precursors of the optic vesicle. Lens placode develops into the lens vesicle. Created with BioRender.com

In mouse, retinal neurogenesis begins at embryonic stage (E) 11 and finishes by postnatal stage (P) 11 (Figure 1.2). Ganglion cells are the first to differentiate from progenitor cells, shortly followed by horizontal cells and cone photoreceptors. These cell types differentiate during the early/embryonic stages and are considered early born cell types (Figure 1.2). Amacrine cells and rod photoreceptors are born during intermediate stages of retinal development, as they span embryonic and postnatal stages, whereas bipolar cells and Müller glia cells differentiate during later/postnatal stages and are considered late-born cells[10–15]. The cell fate decisions made by retinal progenitor cells are firmly governed by an intrinsic genetic program, although the ratio of cell types they produce can also be influenced by extrinsic/environmental cues[16–18].

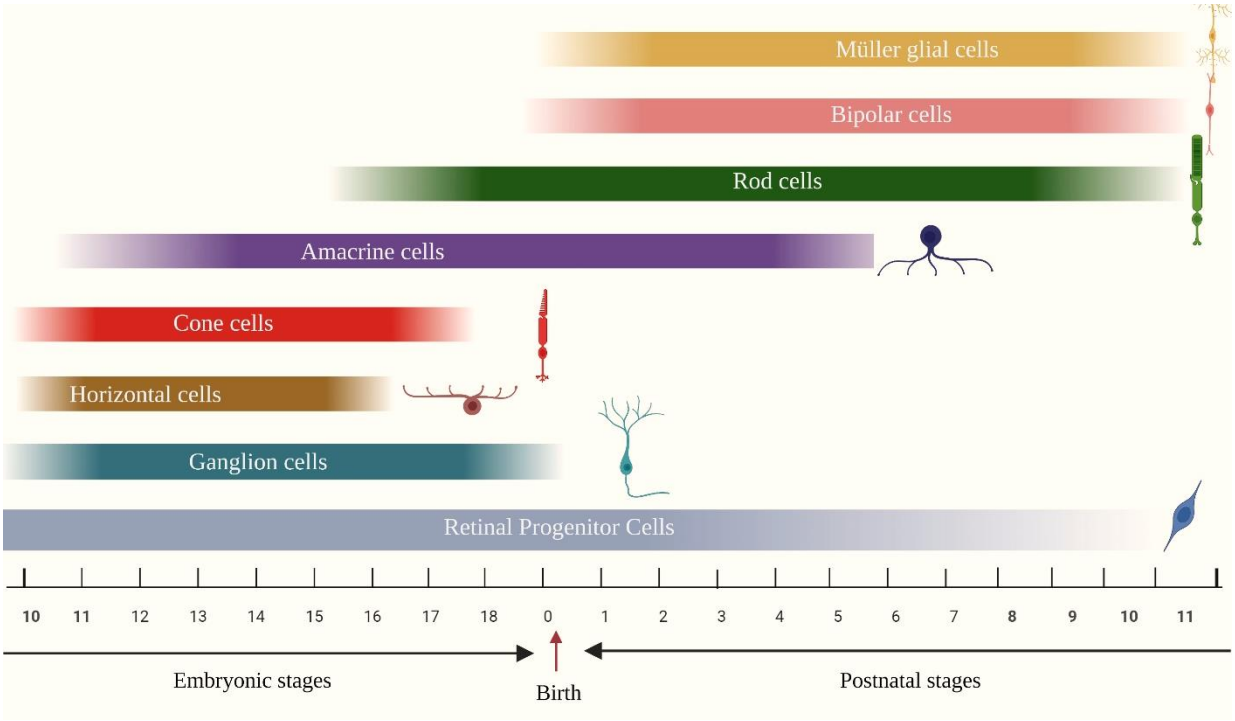

Figure 1.2 Order of different cell types generated during mouse retinal development.

Sequential and overlapping order of retinal cell birth differentiating from retinal progenitor cells (RPCs) during development (embryonic and postnatal timeline). Ganglion cells, horizontals and cones are considered as early born cell types. Amacrines and rods are mid/late born cell types, whereas bipolars and Müllers are considered as late-born cell types. Created with BioRender.com

Vertebrate retinal neurogenesis has been characterized using experiments such as cell fate mapping, clonal analyses, and lineage tracing, revealing that retinal development has the following features. 1) All the cell types are generated from a single pool of multipotent retinal progenitor cells (RPCs)[11,19,20]. 2) Differentiated retinal cell types are generated sequentially, and the order of cell type specification is highly conserved across species[11–13] . 3) Based on how RPCs generate different cell types during retina development, two (non-exclusive) models are proposed- the competence model and the stochastic model. The competence model states that the RPCs are intrinsically programed to undergo sequential changes in competence states. During each change in competence, RPCs progressively gain and lose the ability to differentiate into certain cell types

over the course of development[21]. The stochastic model accounts for the peculiar behaviour of RPCs examined in timelapse experiments. Individual progenitor cells differentiate into clones that vary in size and cell composition. Hence, the developmental progression of RPCs is not always identical. Several lines of evidence support the notion that the lineage progression in retinal development is controlled stochastically; however, it still remains controversial [22–24].

1.1.1 Fully developed/ adult retina structure

Retinal cells are organized into three nuclear layers separated by two synaptic, or plexiform layers (Figure 1.3). The outer nuclear layer (ONL) contains the cell bodies of the photoreceptor cells: rods and cones. The photoreceptors detect photons and convert light into neural impulses. The inner nuclear layer (INL) contains the cell bodies of the horizontals, bipolars, and amacrines which process and transmit information from photoreceptors to the ganglion cells (Figure 1.3). It also contains cell bodies of Müller glial cells but their processes span the entire retina, and support the structure and homeostasis of the retina. The ganglion cell layer (GCL) includes some displaced amacrine cells, and the ganglion cells - whose axons form the optic nerve and project into the thalamus (Figure 1.3).

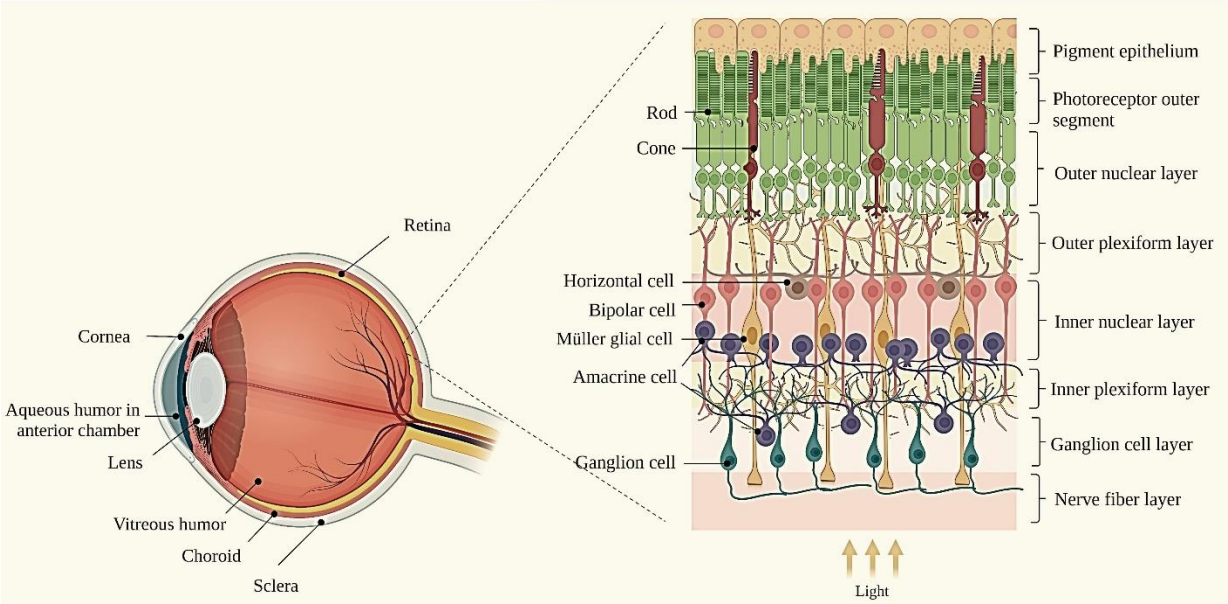

Figure 1.3 Schematic representation of the eye and schematic enlargement of the retina struture

Left- The anterior chamber of the eye is composed of the cornea, the pupil, the iris, and the lens, the posterior chamber is comprised of the vitreous humour, the retina, the choroid and the sclera. **Right**- The retina is divided into three layers: the outer nuclear layer (ONL), the inner nuclear layer (INL) and the ganglion cell layer (GCL). Retinal cells are distributed among these layers: rod and cone photoreceptor cell bodies are in the ONL; the cell bodies of bipolar, horizontal, amacrine and Müller glia, are located in the INL; and the cell bodies of ganglion cells and displaced amacrines are located in the GCL. Ganglion cell axons run just beneath the GCL and comprise a nerve fibre layer (NFL). Synapses between photoreceptors and interneurons form in the outer plexiform layer (OPL), and synapses between interneurons and ganglion cells form in the inner plexiform layer (IPL). Created with BioRender.com

1.1.2 Factors that govern retinal neurogenesis

Genetic Factors

Over the past few decades, studies were performed to understand the role/s of the genetic factors (intrinsic and extrinsic factors) and their contribution for the proper development of the retina[9,25]. Transcription factors are proteins that bind to DNA and control gene expression. Studies have shown that these factors are usually involved in multiple regulatory networks in which they might work together or cross-regulate each other to specify neuronal types in the developing retina[17,26,27].

Their functions include maintaining the balance between the multipotency and proliferative capability of RPCs (Pax6[28], Vsx2[29], Sox2[30] etc.) as well as to control the specification and differentiation of RPCs into mature retinal neurons and glia. The key intrinsic factors involved in retinal neurogenesis belong to the homeodomain-containing gene family, the basic helix-loop-helix (bHLH) family, and the nuclear hormone receptor family. Some of these transcription factors are crucial for cell-type specification during development such as Nrl for photoreceptor development[31], and Atoh7 (Math5) and Pou4f2 (Brn3b) for RGC genesis[32]. The extrinsic factors for cell to cell signalling known to regulate retinogenesis are Sonic Hedgehog[33] (Shh), Notch[34], Fibroblast growth factors[35] (Fgfs), Wnt[36] and retinoic acid[37] (RA). However, while the factors governing cell type identity are well understood, the factors that govern the potential and behaviour of retinal progenitors are not fully understood.

1.1.3 Epigenetic factors:

As only a few transcription factors have been shown to control temporal competence states, epigenome regulators have been proposed as good candidates that might control the developmental potential of RPCs in a cell-intrinsic manner. In addition to transcription factors, there are several epigenetic regulators that can either directly or indirectly influence chromatin accessibility and gene transcription, which adds another layer of complexity to the system. These include nucleosome remodelers, histone modifications, DNA methylation, and non-coding RNAs that have been shown to play a significant role in gene transcription thereby defining the cell type and retinal development[26,38].

1.1.4 Chromatin remodelers:

DNA is tightly packed by proteins – with histones playing a particularly prominent role, thereby forming a complex called chromatin. DNA in its condensed form is inaccessible to DNA-binding

factors (such as RNA polymerase, transcription factors). Chromatin remodelers are protein that can bind to chromatin and alter interactions between histones and DNA thereby altering accessibility at regulatory elements [39]. Chromatin remodelers commonly have an ATPase domain and utilises the energy from the hydrolysis of ATP to reposition and remove nucleosomes. Chromatin remodelers are classified into four families: SWItch/Sucrose Non-Fermentable (SWI/SNF), imitation SWI (ISWI), Chromodomain Helicase DNA Binding Protein (CHD), and INO80.

CHD remodeling complexes are mainly associated with transcriptional repression and for the maintenance of pluripotency[40,41]. Our lab primarily focused on understanding the role of the NuRD complex and its subunits in retinal neurogenesis[42]. In our proteomics of chromodomain-helicase-DNA-binding protein (Chd4), a key subunit of NuRD responsible for its chromatin remodelling activity, surprisingly Adnp, an autism risk gene, was found to be enriched. Interestingly, recent studies suggest that Adnp and Chd4 form a chromatin remodelling complex called ChAHP (CHD4, ADNP, HP1)[43]. Prior work in our lab implicates Casz1 and NuRD in retinal neurogenesis; we wondered whether Adnp might also regulate retinal development. Hence my project is designed to investigate Adnp function in neurogenesis.

1.2 Activity dependent neuroprotective protein

Activity dependent neuroprotective protein (ADNP), a zinc finger and homeodomain transcription factor (Figure 1.4), was identified as a vital gene for embryonic development and brain formation[44]. However, due to early lethality of *Adnp* knockouts, its exact role in neurodevelopment is unclear. It was discovered in a screen for neuroprotective peptides [45]. The active peptide NAP (NAPVSIPQ) of this protein, when added exogenously, showed neuroprotective properties in some disease models[46–49]. Indeed, numerous studies have focused on the activity and production

of the NAP peptide rather than the role of the entire ADNP protein. More studies are needed to understand the role of the Adnp protein. Here, we propose to focus on the role of ADNP in neurogenesis using retina as a model system.

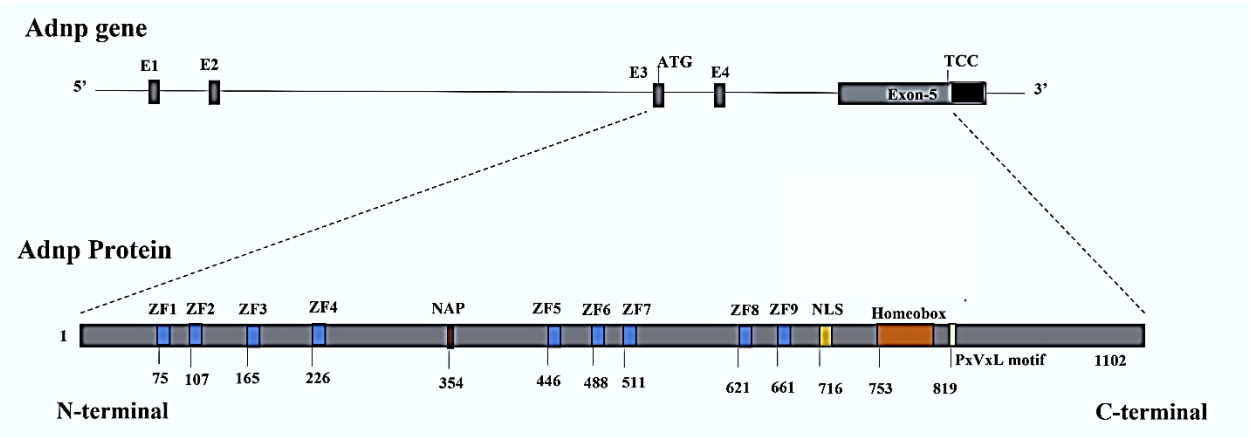

Figure 1.2. Structure of the ADNP gene and functional domains of the ADNP protein

The Adnp gene contains four introns and five exons. As the start codon (ATG) is located on the 3rd exon, only the last three are translated while exon 5 alone contains known functional domains. The Adnp protein comprises 1102 amino acids (aa) and possesses nine C2H2 zinc fingers, a DNA binding homeobox domain and a bipartite nuclear localization signal (NLS) strongly suggesting its role as a zinc finger transcription factor. ZF, zinc figures; NAP, neuroprotective peptide.

1.2.1 Structure of ADNP gene and protein

The *ADNP* gene is located on the long arm of chromosome 20 (20q13.13) in humans[50] and on chromosome 2 in mouse. In humans, the gene is ~40 kilobases long and contains four introns and five exons. As the start codon (ATG) is located on the 3rd exon, only the last three exons are translated while exon 5 alone contains functional domains. The ADNP protein comprises 1102 amino acids and possesses nine C2H2 zinc fingers, a DNA binding homeobox domain and a bipartite nuclear localization signal (NLS) strongly suggesting its role as a transcription factor[50] (Figure 1.4).

1.2.2 *ADNP* mutations and HVDAS/ADNP syndrome

ADNP was found to be among the most prevalently mutated genes associated with autism spectrum disorders (ASDs)[51–53]. Mutations in the *ADNP* gene cause ADNP syndrome or Helsmoortel-Van der Aa syndrome (HVDAS) and *ADNP* is thought to be the 3rd most common single gene among ASD individuals. Moreover, there are twice as many individuals diagnosed with intellectual disability relative to ASD. HVDAS syndrome is an extremely severe condition affecting multiple body systems, suggesting that ADNP has a vital role in overall development. It is characterized by developmental delays, severe intellectual disabilities, vision impairment, motor delays and gastrointestinal problems[54]. In most of the ASD and HVDAS cases, *ADNP* mutations were identified as *de novo*[54,55]. However, the precise mechanisms by which these mutations alter ADNP function are yet to be determined.

1.3 Importance of ADNP in development

1.3.1 Adnp is essential for embryogenesis and neurogenesis

To investigate the role of Adnp in development, a germline knockout (KO) was generated but the mouse embryos died around E8.5-E9 [44] (Figure 1.5). Although, KO mice thus do not mimic HVDAS disease, this study suggested that the gene is essential for embryonic development and crucial for brain formation[44]. Indeed, ADNP is strongly expressed in the brain, compared to the rest of the body. In *Adnp* KO embryos, the expression of the pluripotency marker Oct4 was found to be increased, while the neural progenitor marker Pax6 was found to be absent in the anterior neural plate of the KO mice[44]. A recent study also showed that *Adnp* KO mouse embryonic stem cells (ESc) failed to differentiate into neural lineages, implying Adnp might be crucial for neural induction[43] (Figure 1.5). However, the exact role of Adnp in neurodevelopment is still unclear.

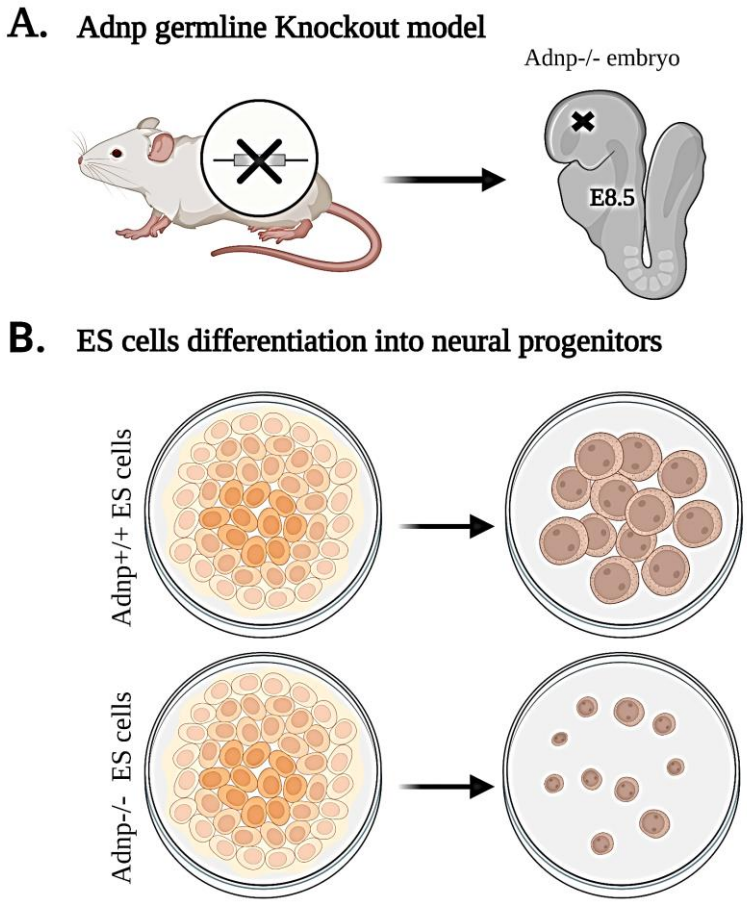

Figure 1.3. Schematic presentation of experiments performed to identify Adnp role

Schematic presentation of germline knockout of Adnp which led to lethality at Embryonic stage E8.5 suggesting Adnp is essential for embryonic development[44] B.) Schematic presentation of wild-type and Adnp KO ES cells that were directed to differentiate and form neural progenitors (NP). Adnp KO cells formed smaller embryoid bodies, demonstrating Adnp is crucial for neural development[43].

1.3.2 Adnp regulates gene expression by its interaction with chromatin binding proteins

Several studies were performed to characterize Adnp protein-protein interactions using a wide variety of cell lines. Initial bioinformatic analysis found a conserved potential heterochromatin protein1α (HP1α) binding the PxVxL motif within the C-terminal region of Adnp[56]. A study on ADNP-deficient embryos and the pluripotent P19 cell line, has reported that Adnp interacts with chromatin through its association with HP1α and thereby controls the gene regulation required for organogenesis/ neurogenesis[57]. Shortly after, ADNP was identified as a member of the SWI/SNF

chromatin remodeling complex[58]. This latter study was performed on HEK293 human embryonic kidney cells and revealed that several subunits of the SWI/SNF complex co-immunoprecipitated with ADNP, including BRG1, BAF250a, and BAF170[58].

More recently, an ADNP-interaction study performed using mouse embryonic stem cells (mESC) identified that ADNP interacts with the NuRD subunit CHD4 and HP1γ to form a stable complex named ChAHP. ADNP and HP1 isoforms (HP1β, HP1γ and HP1α genes) were tagged endogenously with a Flag-AviTag and subjected to tandem-affinity purification coupled to liquid chromatography tandem mass spectrometry (TAP–LC–MS/MS). HP1β, HP1γ and CHD4 interactomes were highly enriched for ADNP peptides. Moreover, in HP1β and HP1γ purification, both ADNP and CHD4 were highly enriched. In contrast to previous studies, no SWI/SNF complex subunits were found in ADNP purifications. ChAHP complex formation was also verified by size-exclusion chromatography (SEC) performed on cells expressing the human recombinant ADNP, HP1γ and CHD4. Importantly, the study found that ADNP interacts with Chd4 outside of its canonical NuRD complex.

Another research group examined the domain architecture of the NuRD and ChAHP complexes[59]. This study performed co-immunoprecipitation on both N and C–terminally Flag-tagged full-length ADNP and CHD4 proteins in HEK293 cells. The N-terminus (ADNP-N, aa1-228) pulled down both full length CHD4 and the CHD4 C-terminal domain (aa 1230-1912) and similarly, HA-CHD4 proteins pull down the ADNP-N construct[59].

A recent study shows that POGZ, another high-risk autism gene, forms a complex with ADNP and HP1γ in the E13.5 mouse cortex[60]. ChIP-seq and RNA-seq analyses revealed a reduced co-occupancy of ADNP, HP1γ, and POGZ near genes that became down-regulated in the *Pogz* knockout. Interestingly, in-situ hybridization has confirmed reduction of *Adnp* mRNA levels in

the *Pogz*$^{+/-}$ cortex. Adnp was also recently observed in the interactomes of TBR1 and ZMYM2/3[61,62]. TBR1 is a neuron-specific transcription factor and was implicated in a neurodevelopmental disorders (NDD). On the other hand, the ZMYM2 is another NDD gene and was involved in silencing of developmentally regulated endogenous retrovirus elements. BioID analysis revealed that ZMYM2 interacts with ChAHP and other epigenetic repressor complexes[61].

1.3.3 Adnp - a multifunctional protein

A growing body of recent research reports Adnp as a chromatin regulator. One study suggests it has a specific role in chromatin looping by competing with CTCF, a loop extrusion anchor[63], and another states it suppresses R loops, three-stranded nucleic acid structures that occur at specific genomic site[64]. In spite of all, most of the studies are performed in different cell lines and no studies have examined the role of Adnp in later stages of neurodevelopment due to lack of appropriate genetic models. More studies are needed to understand the mechanistic role of Adnp during neurodevelopment.

1.4 ADNP and Retina

A detailed clinical characterization of the HVDAS/ ADNP syndrome was performed on a large cohort of individuals with *ADNP* mutations. A wide range of vision problems were identified among the group[54]. A recent ophthalmic study on a HVDAS child reported a range of vision abnormalities such as progressive nystagmus, improper development of the fovea, decreased ratio of inner-to-outer retinal thickness, persistent rod dysfunctions and cone degeneration over time[65]. This study suggests that HVDAS children may also possess retinal dysfunction in addition to refractive or cortical impairments [65].

1.5 Conditional Knockout Mouse Models (cKO)

Genetically modified mouse models are commonly used for modelling human diseases. However, gene knockout studies cannot permit such investigations if the gene of interest is crucial for embryonic development or if its functionality is vital in multiple tissues.

A widely used technique is to generate a conditional knockout model, particularly to investigate a single gene function in a specific tissue/cell type and/or time specific manner[66]. This system utilizes the Cre (Causes recombination) enzyme to precisely cut out the genetic sequence between two LoxP (Locus of crossover P1 bacteriophage) sites[67–70] (Figure 1.6). Due to its efficiency in manipulating genes and chromosomes it has been widely used in mouse genetics. Cre recombinase is a 38kDa site-specific recombinase enzyme derived from P1 bacteriophage[66]. The LoxP site consists of 34 bp sequences that includes 2 symmetric 13bp sequences and 8bp of asymmetric sequence. Based on the orientation and location of loxP sites, Cre recombinase can catalyze the deletion, inversion, or translocation of the LoxP flanked (floxed) DNA sequence[71].

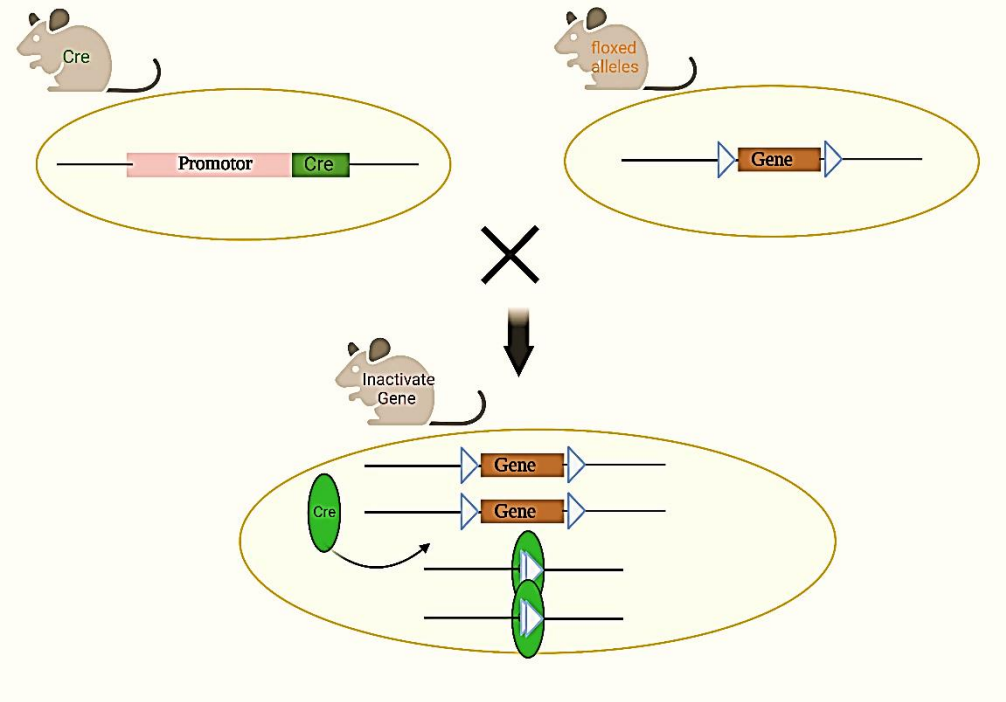

Figure 1.4 Schematic representation of cre-loxP system and inactivation of a specific gene.

General breeding scheme for conditional knockout of specific genes in progeny using Cre-loxP system. In principle, one mouse must have a tissue specific Cre driver, and another must have loxP flanked alleles. In progeny, when Cre is active, it enters the nucleus, binds and recombines the loxP sites thereby inactivating the gene of interest.

Transgenic mice are generated by inserting the foreign gene randomly into the genome. To overcome limitations such as the position effects of integration and transgene size, artificial chromosome type vectors (YACs, BACs and PACs) have been used to generate transgenic mice models over the last two decades[72]. To understand Adnp's role in retinogenesis, we needed Cre mice that can mediate Cre excision specifically in the retina, and not elsewhere within the body. To generate a retina specific knockout, there are several Cre mouse lines that express Cre recombinase in retinal progenitor cells. *Foxg1-Cre* mice showed Cre excision only in the anterior optic vesicle of the retina, but additionally express Cre throughout the forebrain[73]. The *Pax6-αCre* mouse line expresses Cre activity only in the periphery of the retina[74]. In the *Rx-Cre* mice, Cre

mediated excision was observed in E8.5 and in all retinal progenitor cells, however Cre was also strongly expressed in forebrain and hypothalamus[75]. Since germline *Adnp* knockouts were shown to be embryonic lethal, we considered Cre mice that drive excision specifically in the retina. Therefore, we used the *Chx10-Cre* mouse line in which the Cre activity was detected at E10.5[76]. The *Chx10-Cre* transgenic mice have been widely used to generate retina specific knockouts and to study functions of specific genes in retinal development and disease.

1.6 Project objectives

We hypothesize that *Adnp* might have a crucial role in retinal neurogenesis. We aim to 1) investigate the role of Adnp in retina neurogenesis, and 2) identify the putative interacting partners of Adnp. To the best of our knowledge, no studies have investigated the mechanistic role of ADNP in neurogenesis nor its potential role in visual impairment identified in HVDAS children. Thus, this study will address the importance of Adnp in neurogenesis and retinal development.

CHAPTER 2 MATERIALS AND METHODS

2.1 Generation of *Adnp* conditional knockout mice using Cre-LoxP recombination system.

Two mouse strains are needed for the Cre-LoxP system. Chx10-Cre BAC transgenic mice were used to specifically drive Cre excision in the retina[76]. Chx10 (Vsx2) is one of the earliest markers expressed in RPCs and was detected at E9.5 in distal optic vesicle[77]. The BAC reporter contains a GFPCre fusion protein and is expressed under the control of endogenous Chx10 regulatory elements. The Enhanced green fluorescent protein (EGFP) was strongly expressed in retinal progenitor cells during development. The retina-specific *Chx10-Cre* mice were obtained from Dr. Picketts' lab.

Adnp floxed mice were generated by Biocytogen. In mice, Adnp gene spans 26.15 kb on chromosome 2 reverse strand. The *Adnp* gene contains 5 exons: Exon 1 and Exon 2 are in the 5' untranslated region (UTR). The initiation/start codon (ATG) is on the 3rd exon, and the last three exons are translated. Exon 5 alone contains all of the annotated functional domains and encodes for the majority of the Adnp protein.

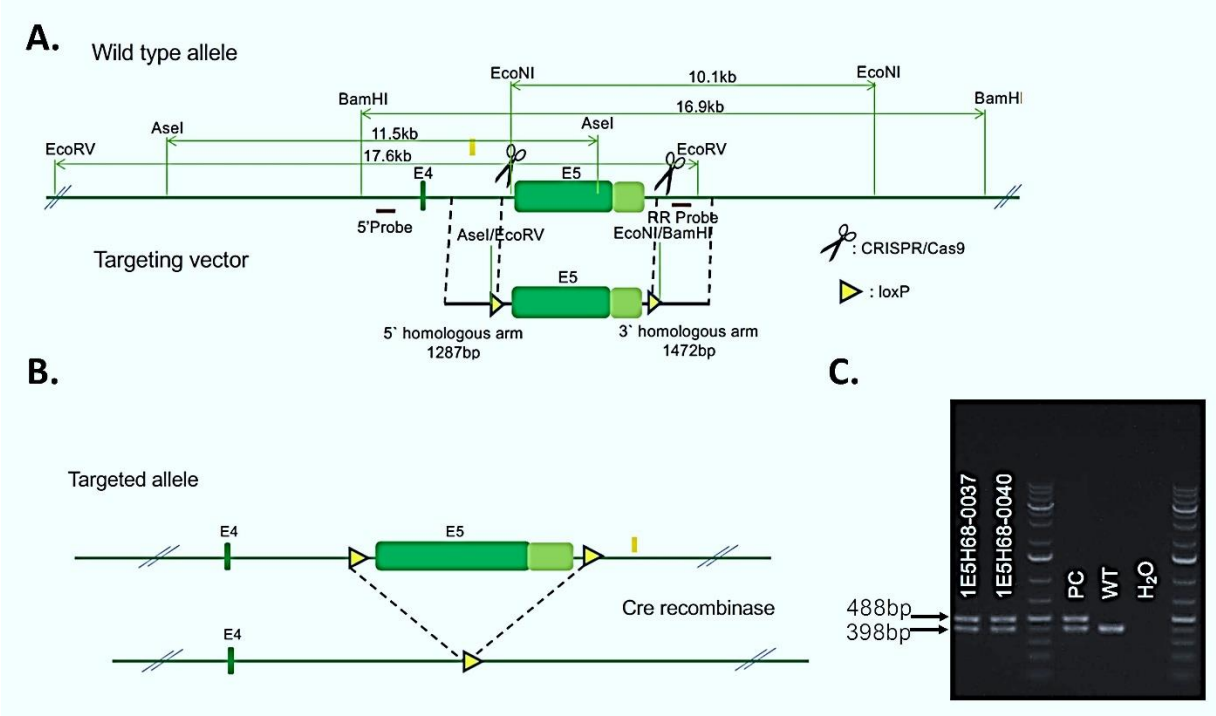

Figure 2.1: Generation of *Adnp* floxed mice

A.) Schematic presentation of mouse *Adnp* gene (exon 5) and the targeting vector. The dotted diagonal stripes indicate the positions of the 5'and 3' flanking sequences used in the targeted vector. Exons (closed boxes), Southern blot probes (Brown lines), *loxP* (yellow arrowheads) are indicated. Sizes of relevant *Eco*RV, AseI, BamHI and EcoNI restriction endonuclease bands are shown in kilobase pairs (kb). sgRNA/ Cas9 (scissors) are the sites, cas9 bind and cut the DNA for insertion of loxP sites. B.) Schematic representation of Cre recombination activity. Cre binds to loxp sites knocking out the targeted Exon5 region of Adnp. C.) The genotyping of F1 heterozygous mice as determined by PCR amplification of genomic DNA. 3'loxp primers were used. The PCR product with no loxP sites/wildtype allele is 398bp. With loxp sites, it is 488bp. The PCR product from heterozygous mice shows two bands, while the product from homozygous mice will show one band. PC-positive control; WT-wildtype; H_2O- water, negative control

To ensure the inactivation of Adnp, loxp sites were inserted on either sides of exon 5 using the CRISPR/Cas9 system (Figure 2.1). The targeting construct with inserted loxP sites was then introduced into ES cells and positive clones were tested for homologous recombination by Southern blot analysis and Restriction digestion. Positive ES cells were microinjected into C57BL/6N zygotes. The offspring were genotyped using 5'loxp and 3'loxp primers to ensure the integrated loxp site in the genome. The chimeric offspring were backcrossed with C57BL/6N mice. The successful germline transmission of the $Adnp^{flox}$ allele was confirmed by PCR product

sequencing and Southern blot analysis (Figure 2.1 and not shown). Heterozygous mice (*Adnp*$^{flox/+}$) were crossed with *Chx10-Cre* mice to produce wildtype (WT), conditional heterozygous (cHET) and conditional knockout (cKO) progeny (Figure 2.2).

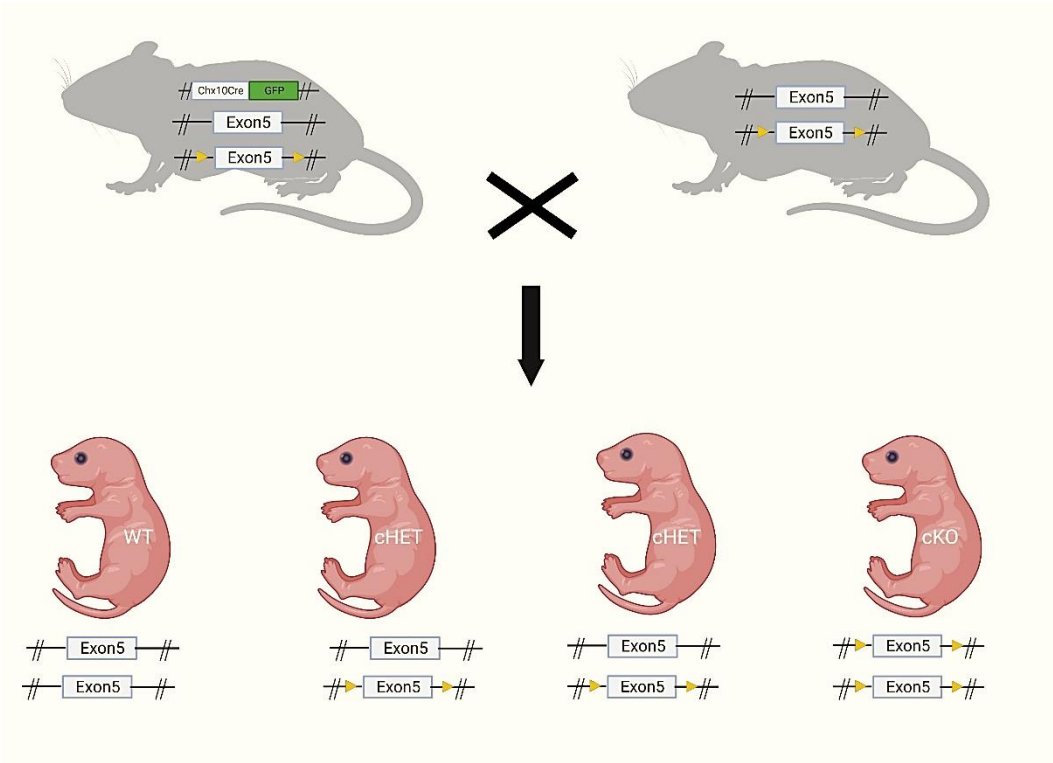

Figure 2.2. Breeding strategy of Cre-loxp mediated recombination and generation of Adnp conditional knockout in mouse retina

Adnp flox/+ mice were crossed in which one parent contains Chx10Cre. The progeny contains a 1:2:1 ratio of WT, cHET and cKO. The Chx10Cre driver is activated around E10.5-E11. It recombines the loxP sites and inactivates the *Adnp* gene specifically in retina. Hence the cKO retina develops in absence of Adnp.

2.2 Genotyping of Chx10-Cre litters

Genomic DNA was isolated from tail samples of individual animals. 120 µl of 50mM NaOH was added to each sample and boiled at 95°C for 20 minutes. 30 µl of 1M Tris Buffer at pH 7.5 was added to neutralize samples and centrifuged at maximum speed (14000 rpm) for 5 minutes. 20 µl

PCR reactions were set up: 10 µl 2x PCR Taq mix (FroggaBio); 1 µl primer (F and R 10 µM each). The PCR program had an initial denaturation step for 5 mins at 95°C followed by 30 cycles, where cycles consisted of 95°C for 30 seconds, (56°C – Adnp3loxp and 65°C – Chx10 Cre) for 60 secs and 72°C for 30 secs and a final extension step for 30 mins. Primers are listed in Table 2.1. The PCR samples were loaded in 1% agarose gels. Electrophoresis was run at 110 V for 45 min. With 3'loxP primers, we find WT PCR product has one band at 398bp and cHET have two bands, while cKO PCR product has one band at 488bp. With Chx10-Cre or Cre primer sets, presence of a single band indicates Cre+, and no band is considered as Cre-.

Table 2.1 Primers used for Genotyping

Adnp 3loxP Primer Forward	TGGCGTAACAGTAAAGGAGAAGTAC
Adnp 3loxP Primer Reverse	AGAGCTTCAGCATGACTTCCAGGTG
Chx10 -Cre Primer Forward	GGGCACCTGGGACCAACTTCACGA
Chx10 -Cre Primer Reverse	CGGCGGCGGTCACGAACTCC

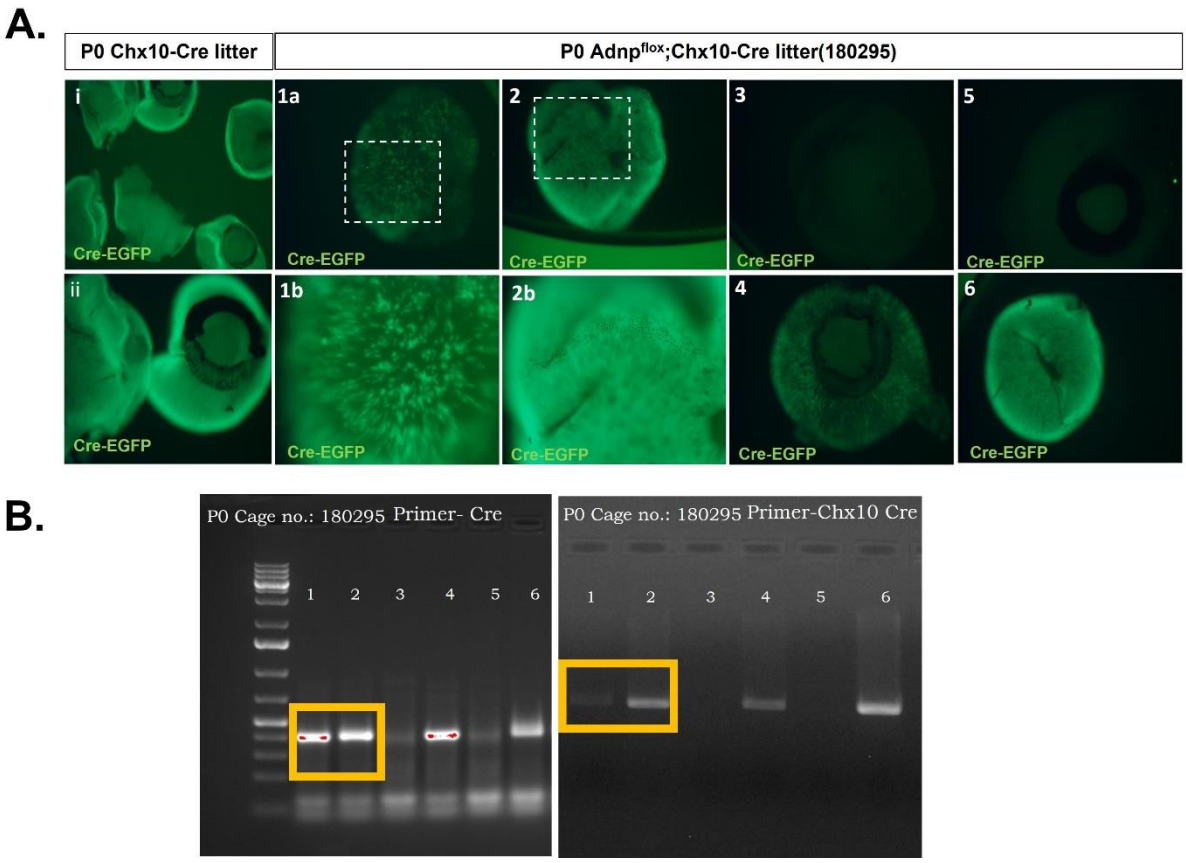

Figure 2.3 Mosaic expression of Cre/EGFP identified in *Adnp*^{flox} Chx10-cre litters.

A) Fluorescence images of Cre/EGFP expression in P0 dissected retinas from a Chx10-cre+ wildtype litter (i-ii) and *Adnp*^{flox}; Chx10-cre litter (1-6). (1b, 2b) zoomed images of rectangle boxes of 1a and 2a images. (3,5) Cre- retinas (1,2,4,6)- mosaic Cre+ retinas- uneven/patchy expression of Cre/GFP. B.) Genotyping of *Adnp*^{flox}; Chx10-cre litter. Genomic DNA was extracted from the mouse tail samples. PCR was set up with Cre and Chx10-Cre primers and PCR products were loaded in 1% Agarose gel then subjected to agarose gel electrophoresis. With Cre primers, presence of a single band indicates Cre+, and no band is considered as Cre-. We found strong band in 1,2,4,6 PCR samples. However, with Chx10-Cre primer set, we found faint bands that recapitulates the mosaic expression of EGFP as seen in fluorescence images suggesting copy number of Chx10-Cre varies in the genome. For instance, presence of strong band with cre primers was observed for both 1 and 2 samples (yellow box) whereas, sample 1 has a very faint band when genotyped specifically for Chx10-Cre in comparison to sample 2 (yellow box). Similarly, the mosaic pattern of pup1 was prominent than Pup 2 in fluorescent images. we used Chx10-Cre for genotyping to identify the mosaic animals.

2.3 Retina preparations for Cryosectioning

2.3.1 Eyecups

Animals were euthanized with carbon dioxide (CO_2) followed by cervical dislocation (P21 mice). Mouse eyes were enucleated using curved forceps and were placed immediately in dissection petri dishes filled with 1x phosphate-buffered saline (PBS). Using forceps, a small incision was made just at the limbus of the eye and a circumferential cut was made to remove the cornea and to extract the lens. The retinas were thereby better exposed to the fixative.

2.3.2 Dissected retina with lens

P0 pups were anesthetized on ice, followed by decapitation. Heads were placed immediately in dissection petri dishes filled with 1X PBS. The eyes were enucleated using curved forceps and transferred into fresh 1X PBS. Using forceps, first a small incision was made just at the limbus of eye, and then cornea and retinal pigmented epithelium surrounding the retina were removed carefully leaving behind the retina intact with lens.

2.4 Tissue fixation and Cryo-sectioning

Eye cups/dissected retinas were fixed in 4 % paraformaldehyde (EM grade, Electron Microscopy Sciences) for 1-2 mins at room temperature (RT) in 1x PBS. After fixation, they were washed 3 times with 1x PBS for 3mins each on a platform shaker and followed by overnight incubation in 20% sucrose in 1x PBS at 4°C. The retinal tissues were then embedded in optimal cutting temperature (OCT) in 10 x 10 mm cryomolds and then stored at -80°C. Tissue sections were cut at 12 um thick using a CM1860 Leica cryostat at −20°C and were carefully transferred to a Superfrost microscope slide (Fisher) by tapping the slide to the tissue.

2.5 Immunohistochemistry and Imaging

Slides were placed in Sequenza slide racks and washed 3 times with 1X PBS to remove the OCT. Next, retinal sections were incubated in Blocking solution (1X PBS; 0.4% Triton X-100 (Bio Basic); 1:5000 Hoechst (Novus); 0.3% BSA (Bio Basic)) for 5 min at RT. Primary antibodies were diluted in the same blocking solution and were added to the slides. Retinal sections were incubated overnight at 4ºC. Later, the retinal sections were washed 3 times by adding 1X PBS (10mins each) to remove the excess primary antibody and followed by secondary antibody staining. Similarly, fluorescent-labeled secondary antibodies were diluted in blocking solution and added to the slides for one hour at RT. Antibodies and dilutions are listed in Table 2.2 and Table 2.3. The retinal sections were then washed 3 times with 1xPBS, each for 10 min. Slides were carefully removed from the slide rack and coverslips were mounted using Mowiol mounting medium (24% Glycerol (Bio Basic); 9.6% Mowiol (Sigma); 0.1M Tris-Cl (pH-8.5) (Fisher)). Keeping the slide flat, slides were allowed to harden slowly by storing them at 4°C. Fluorescent staining was visualized and imaged using a Zeiss LSM 900 confocal microscope.

Table 2.2: Primary antibodies used for immunostaining

Primary antibody	**Species**	**Dilution (µL)**	**Manufacturer**	**Catalog #**
Anti-Adnp	Goat	1:200	R&D systems	AF5919
Anti-Pax6	Rabbit	1:100	Novus	NBP2-19711
Anti-Sox2	Goat	1:100	R&D systems	AF2018
Anti-Otx2	Goat	1:100	R&D systems	AF1979
Anti-Calbindin	Mouse	1:100	Proteintech	66394-1-Ig

Anti-RBPMS	Guinea pig	1:100	Millipore	ABN1376
Anti-Cone Arrestin	Rabbit	1:100	Millipore	AB15282
Anti-Caspase3	Rabbit	1:100	Cell Signalling	9664T
Anti-Chd4	Mouse	1:100	Abcam	AB70469
Anti-Brg1	Mouse	1:100	Cell Signalling	72182S
Anti-Pogz	Rabbit	1:100	Bethyl Laboratories	A302-510A-T

Table 2.3: Secondary antibodies used for immunostaining

Secondary antibody	**Species**	**Dilution**	**Manufacturer**	**Catalog #**
Anti-Rabbit IgG(H+L) Alexa 647	Donkey	1:1000	Jackson Immunoresearch	711-607-003
Anti-Rabbit IgG(H+L) (DyLight 549)	Donkey	1:1000	Rockland	611-742-127
Anti-Guinea pig IgG(H+L) Alexa555	Donkey	1:1000	Thermo Scentific	A-21435
Anti-Goat IgG (DyLight 550)	Donkey	1:1000	Bethyl Laboratories	AA50-101D3
Anti-Mouse IgG(H+L) (DyLight 549)	Donkey	1:1000	Rockland	610-742-124
Anti-Mouse IgG(H+L) (DyLight 649)	Donkey	1:1000	Rockland	610-743-124

2.6 Cell Counting and analysis

Manual cell counting was performed on CZI images (Zen, Zeiss) using Fiji (ImageJ version 1.53t). The images were opened directly in Fiji. Each individual channel was merged before cell counting and using the rectangle selection tool, cells within 100 microns (along the tangential axis) were counted for all the cell markers. Using the Multipoint tool, each cell was labelled by clicking on it and was assigned numbers starting from 1. Sections were counterstained with Hoechst to identify nuclei of cells. Cells stained for each cell-type marker and Hoechst were counted separately. The counts for each cell type and total cells in 100 microns for four sections per retina were saved in Excel (Microsoft) spreadsheets. I have analyzed P21 retinas from WT Cre+ve (n=2), WT Cre-ve (n=1), cHETs (n=3) and cKOs (n=4). For each retina, means were calculated for cells counted in four sections using Excel (Microsoft). Replicate means were averaged and the standard error of mean (SEM) was calculated and graphed, again using Excel. The data was analysed, and the graphs were plotted using GraphPad Prism version 7.0 statistical software.

2.7 Co-immunoprecipitation assay (Co-IP)

Retinal tissues were dissected from eyes of the wild-type animals (8 animals/16 retinas) and immediately transferred into ice-cold radioimmunoprecipitation assay (RIPA) lysis buffer (150mM NaCl; 1% NP-40; 0.5% deochycholate; 0.1% SDS; 1M Tris (pH:8.0)) that contained protease inhibitors (1X Complete (Roche)) to prevent degradation. Samples were subjected to sonication (2 pulses: 6 secs each) and followed by centrifugation (14000 x g; 5mins at 4°C) to remove the cell debris. The supernatant/ protein sample (considered as INPUT) was carefully transferred into new Eppendorf tubes. For each immunoprecipitation (IP), equal amount of protein samples was used, and IP IgG was used as the negative control. For each IP reaction, 1 µl of

antibody (protein of interest), 30 µl of Protein A/G paramagnetic beads (Cell Signalling) were added to each protein sample. IPs were incubated overnight at 4°C on a rotator with gentle agitation. Next, the samples were transferred into new tubes and using magnets, beads were washed three times with RIPA lysis buffer to remove non-specific binding. To elute the proteins, 10 µl of 4x loading dye was added to the beads, and samples and were heated to 94°C for 10 mins. The eluted proteins in dye were ready to load in SDS-PAGE gels.

2.8 Westerns and SDS-PAGE gels

For the western experiments, 10% SDS gels (40% Acrylamide/bis (Bio Basics), 1.5 M Tris (pH-8.8) (Fisher), 10% (w/v) SDS (Fisher), 10% (w/v) APS (Bio Basics), 0.1% TEMED (Fisher), ddH_2O)) were used. For Co-IP experiments, a 10:8:6 % gradient gel with a 4% Stacking gel were used. Samples were loaded along with the protein ladder (Bio-Rad), controls and subjected to gel electrophoresis to separate the proteins based on their molecular weight. Electrophoresis was run at 110 V for 90 min. Proteins were transferred onto polyvinylidene fluoride (PVDF) membranes using Trans-Blot Turbo transfer system (Bio-Rad). Membranes were then fixed in 100% ethanol and let dry for future use or incubated in blocking solution (3% skimmed milk, 20 mM Tris, 150 mM NaCl, pH 7.5 with 0.05% Tween®-20) before probing with antibodies. Primary and secondary antibodies were listed in table 2.4 and 2.5. To visualize proteins, we used commercially available Clarity western ECL kits (Bio-Rad) for enhanced chemiluminescence, and images were obtained using a ChemiDoc (Bio-Rad) at exposure time 300 secs. Protein quantification was performed on western blots using Fiji (ImageJ version 1.53t). For protein expression analysis, protein/actin ratios were measured for control and cKO groups.

Table 2.4: Primary antibodies used for westerns and CoIPs

Primary antibody	Species	Dilution (µL)	Manufacturer	Catalog #
Anti-Adnp	Goat	1:1000	R&D systems	AF5919
Anti-Chd4	Mouse	1:1000	Abcam	AB70469
Anti-Brg1	Mouse	1:1000	Cell Signalling	72182S
Anti-Pogz	Rabbit	1:1000	Bethyl Laboratories	A302-510A-T

Table 2.5:Secondary antibodies used for westerns and CoIPs

Secondary antibody	Dilution (µL)	Manufacturer	Catalog #
Anti-Goat HRP	1:10000	Invitrogen	A16005
Anti-Mouse HRP	1:10000	GElifesciences	NA931
Anti-Rabbit HRP	1:10000	GElifesciences	NA934

CHAPTER 3: INVESTIGATE THE ROLE OF ADNP IN RETINAL NEUROGENESIS

3.1 Assessment of Adnp expression in the developing mouse retina

To better understand the role of *Adnp* in retinal development, we first examined Adnp expression at different embryonic stages: E11, E13, E17 (Figure 3.1 A-F), postnatal developmental stages: P2, P7, P10 (Figure 3.1 G-N) and at P21/ adult stages (Figure 3.1 O-R). Adnp was expressed ubiquitously in retinal progenitor cells (RPCs) from the earliest developmental stage examined (E11). However, its expression was particularly high in postmitotic cells as observed in the GCL of E17 and P2 developmental stages. At late developmental stages (P7, P10), Adnp was expressed in all retinal cell types. Indeed, Adnp expression was maintained in all the cell types of adult/P21 retinas. The expression of Adnp protein in all retinal cell types suggests that Adnp could have important functions in progenitors, neurons and glia.

3.2 Generation of *Adnp* conditional knockout mice using Cre-loxP system

Previous studies have shown that the germline *Adnp* knockout causes lethality in mouse embryos at approximately E8.5[44]. Therefore, our objective was to generate an appropriate model to study the role of Adnp in retinal neurogenesis using the Cre-loxP recombination system. Thus, we crossed *Chx10-Cre* mice[76], which express Cre recombinase in all RPCs beginning at E10.5, with *Adnp* floxed mice to generate a retina-specific conditional knock-out model.

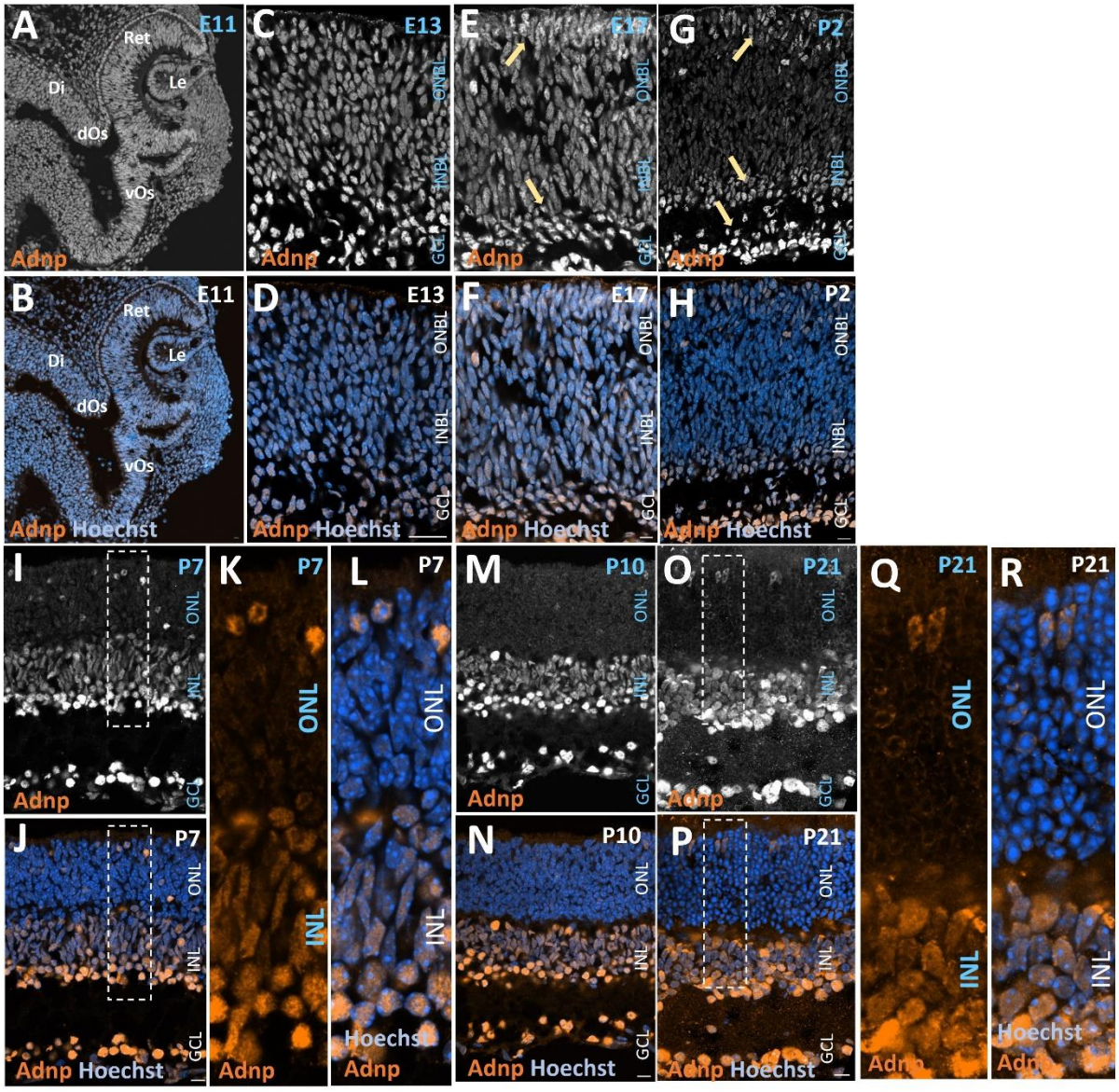

Figure 3.1 -Expression pattern of Adnp in the developing and adult mouse retina.

Retinal cryosections were immunostained with anti-Adnp (orange) and the nuclei were counterstained by Hoechst (fluorescent stain; blue). (A-F) Adnp expression at different embryonic stages (E11, E13, E17). (G-N) Adnp expression in different postnatal stages (P2, P7, P10). (O-R) Adnp expression in adult/ P21/ fully developed retina. Adnp expression is particularly high in differentiated cells (yellow arrow pointing at differentiated cells in E and G). (A,C,E,G,I,M,O) Adnp expression in grayscale. Dashed boxes indicate inset regions in K, L, Q, R. ONBL, outer neuroblastic layer; INBL, inner neuroblastic layer; ONL, outer nuclear layer; INL, inner nuclear layer; IPL, inner plexiform layer; GCL, ganglion cell layer. Scale bars, 10 μm.

3.2.1 Assessment of Cre-loxP recombination efficiency

We investigated whether the *Chx10-Cre* driver can mediate the recombination at loxP sites and conditionally ablate *Adnp* in the retina. Retinas from *Adnp*^{flox}; *Chx10-Cre* litters were dissected, sectioned and processed for anti-Adnp immunostaining. If the Cre- mediated excision is effective, we expect a loss of Adnp expression. In the Cre negative control animals, Adnp staining was visualized in all cells of the retina as expected. On the other hand, I observed a severe decrease in Adnp staining in conditional knockout retinas compared to controls (Figure 3.2A).

3.2.2 Mosaicism associated with Chx10-Cre mouse line

The *Chx10-Cre* transgenic mouse line has mosaic expression of Cre and to an extent that has been previously described[76]. We initially had breeding cages that generated animals with mosaic Cre expression on a sporadic basis (that were excluded from analysis). However, subsequent breeding cages exhibited extensive mosaicism. This might have happened because if/when mosaic animals were selected for subsequent breeding, the mosaicism could not revert back to the normal expression pattern in the offspring. In the mosaic retinas, stripes of Adnp-negative/GFP+ (ie. knocked-out) RPCs were present next to stripes of Adnp+/GFP-negative cells (ie. not knocked-out; Figure 3.2B). The *Chx10*-BAC expresses a GFP-Cre fusion protein and cells that expressed GFP-Cre had evidently lost Adnp expression in mosaic retinas. These data suggest that *Chx10-Cre* efficiently mediates excision of Adnp in RPCs and also validates the specificity of the Adnp antibody. However, mosaic animals would be unsuitable for phenotyping, as Adnp+ and Adnp-negative cells would be intermixed at adult stages (but GFP-Cre would no longer mark all of the recombined cells). To overcome/limit the mosaicism, breeding strategies were handled meticulously to generate cKO animals. After repeated genotyping, we set up new cages with animals which had good expression of the Chx10-Cre. I finally got cKO animals which had ~90% of cells that

lacked Adnp expression as visualized by immunofluorescence. I also performed western blot analysis using P0 retinas of animals from new breeding cages and confirmed that the Adnp protein was almost completely lost in cKO animals from new cages (see Figure 4.3).

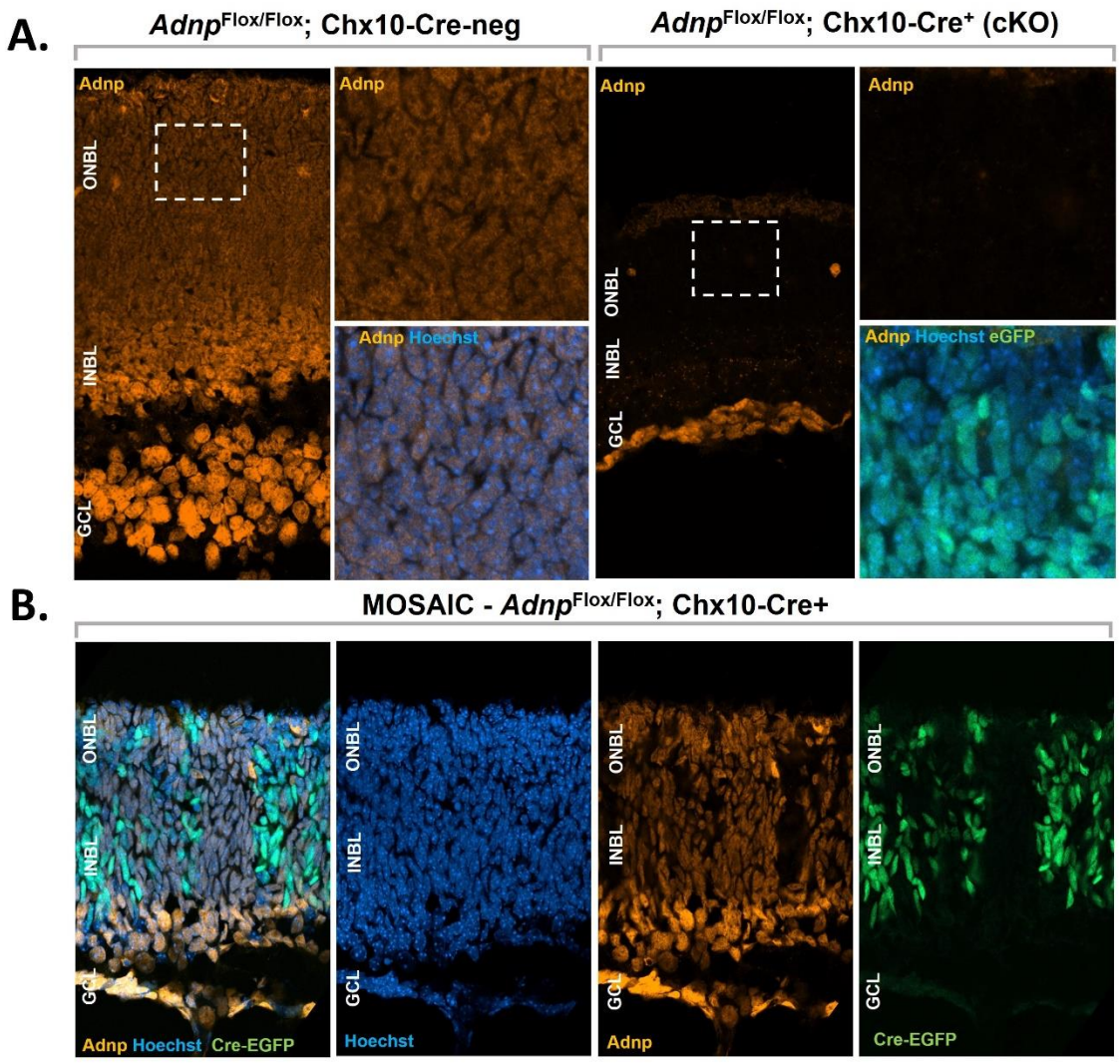

Figure 3.2 Adnp expression was lost in GFP+ RPCs

A.) Adnp staining on P3 WT and cKO retinas. Adnp protein (orange) is expressed in all retinal cells, potential retinal progenitor cells of ONBL as well as in differentiated cells of INBL and GCL in Cre negative/ control retinas. Whereas in the cKO retina (right), Adnp expression was lost in ONBL and INBL cells. B.) Adnp immunostaining on the mosaic retina. The Adnp expression was similar to controls, but it was evidently lost in stripes of Cre+ cells.

3.2.3 Impact of Adnp inactivation on retinal development

To investigate the impact of Adnp inactivation on retinal development, I performed Adnp immunostaining on the adult/P21 retinas of three genotypes (WT, cHET and cKO) from *Adnp*^{flox}; Chx10-Cre cages. As expected, the Adnp expression was significantly lost in retinal cells of cKOs

whereas Adnp was strongly expressed in cells of both WT and cHET retinas (Figure 3.3). No phenotypic changes were identified in *Adnp*-cHET retinas but interestingly the cKO retinas exhibited a clear reduction in overall size of the retina (Figure 3.3). This suggests that the loss of Adnp causes retinal hypoplasia.

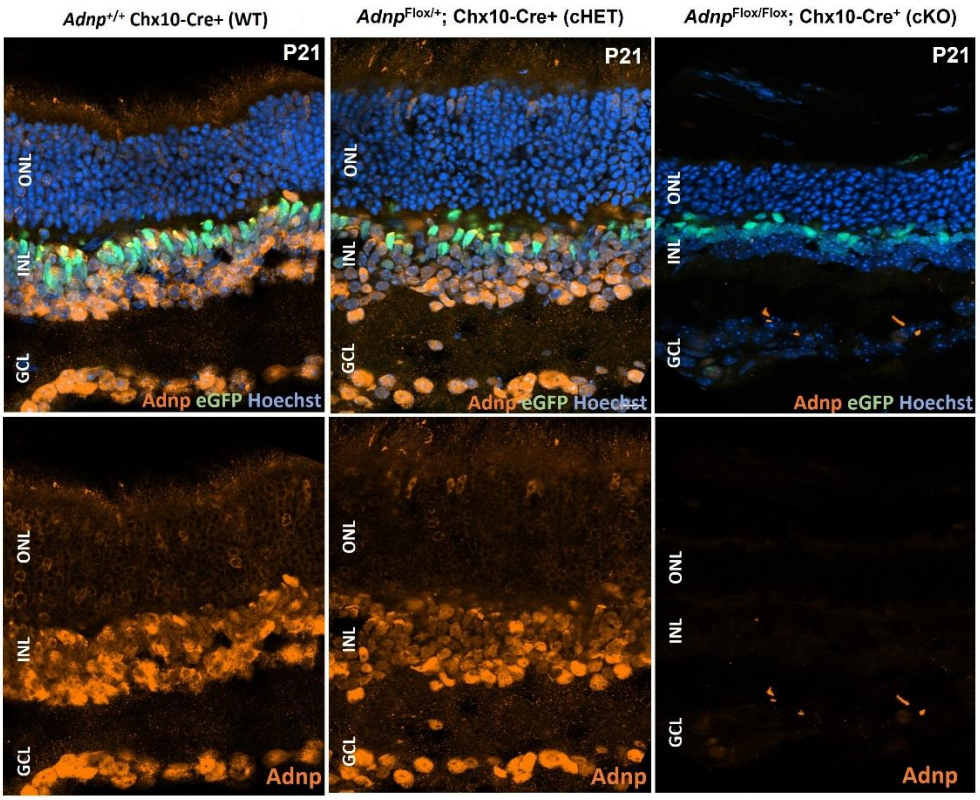

Figure 3.3 Adnp expression was almost lost in cKO retina.

Adnp staining on P21 WT (Cre+), cHET and cKO retinas: Adnp (orange) is expressed in all retinal cell types in both WT-Cre+ and cHET retinas. By contrast, in cKO retinas, Adnp expression was almost completely lost. Hoechst (blue) stains the nuclei of cells and GFP is observed in bipolar and Müller glial cells to which Chx10 expression is restricted at this stage. No morphological changes were observed in cHETs, whereas cKO retinas were smaller in size.

3.2.4 Decreased number of cells in ONL and INL of cKO retinas.

In order to determine how Adnp mutation affected retinal cell numbers, WT (Cre+ve n=2; Cre-ve n=1), cHETs (n=3) and cKOs (n=4) were analyzed. Four cryosections from the peripheral retina (technical replicates) were imaged and cell counting was performed. I first examined the absolute

and proportional cell counts for each layer: ONL, INL and GCL for the three genotypes. The absolute cell numbers within the ONL and INL were significantly decreased in cKO retinas compared to WT and cHET retinas (Figure 3.4B). However, the proportion of cells within each layer of cKOs and controls (WTs and cHETs) were surprisingly similar (Figure 3.4C).

Since there was no difference between WTs and cHETs in overall cell numbers, I pooled them as controls. I also compared WTs versus cHETs for the cell type-specific counts (below), but did not see any obvious difference in numbers, which further justified pooling them together. Next, I investigated whether Adnp loss altered the cell composition of cKO retinas. To do so, I performed histological analysis using cell-type markers and performed both absolute cell counts as well as proportional analysis (Supplementary Figure 1) for rods, cones, bipolar cells, amacrines, and Müller glia cells.

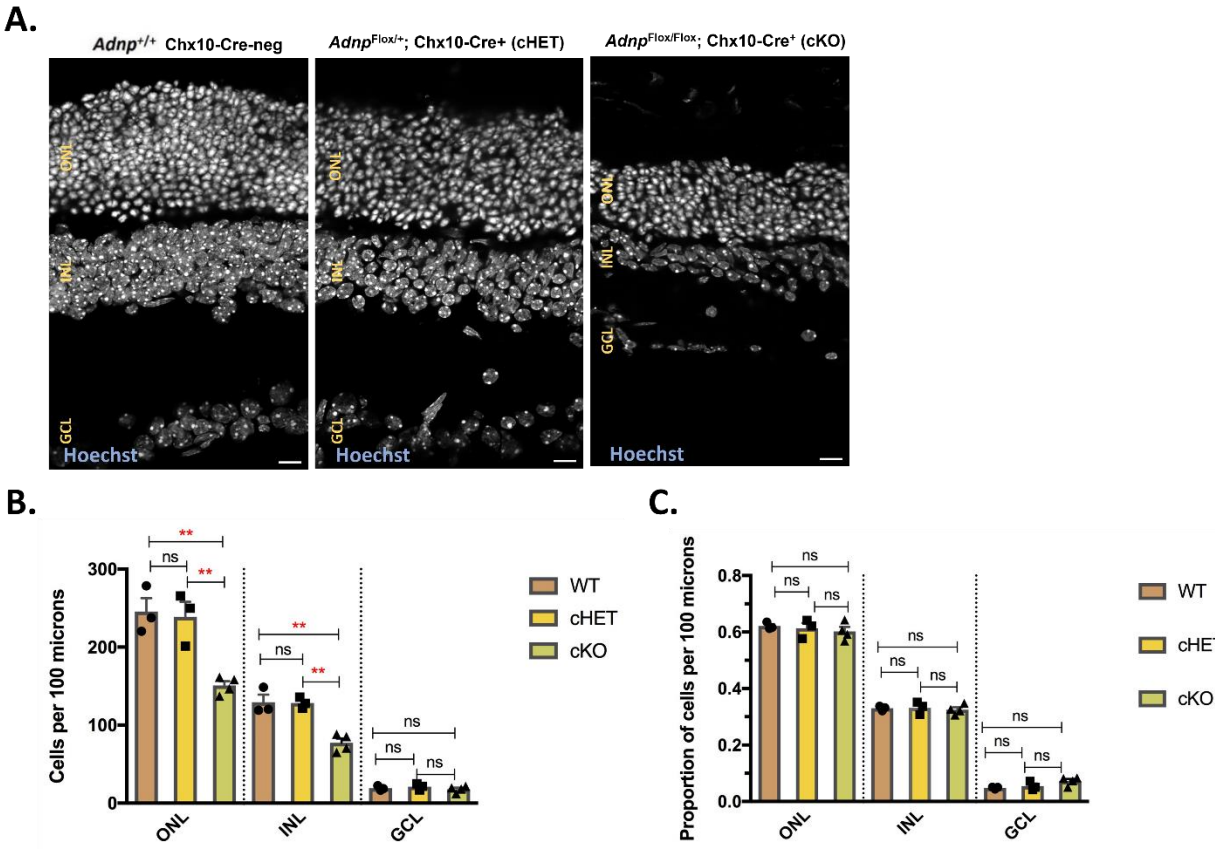

Figure 3.4 Adnp loss resulted in fewer cells in ONL and INL.

A.) Frontal sections of the WT, cHET and cKO retinas at P21 stained with nuclear marker/Hoechst fluorescent dye. cKO retinas were considerably smaller than wild-type and cHET retinas. B.) Absolute cell counts of the three nuclear layers in WT vs cHET vs cKO retinas. Cells in ONL and INL were significantly reduced in cKO compared to WT and cHET retina. C.) Proportional analysis of cell counts of three nuclear layers of WT vs cHET vs cKO. Proportional analysis showed no statistically significant difference between WT, cHET and cKO groups. Statistical analysis was performed using One-way ANOVA, * $p < 0.05$. ** $p < 0.02$

3.2.5 Significantly reduced numbers of photoreceptor cells in cKO retina

In the murine retina, cone arrestin is specifically expressed by cone photoreceptors and absent in rod photoreceptors[78]. To examine whether Adnp loss affected photoreceptors, I performed cone arrestin staining on P21 retinal sections (Figure 3.5A) and counted both cone and rod photoreceptors in the ONL/ photoreceptor layer. There was a significant decrease in cones, while rod cells were drastically decreased in absolute numbers in the cKO retina (Figure 3.5B, 3.5C).

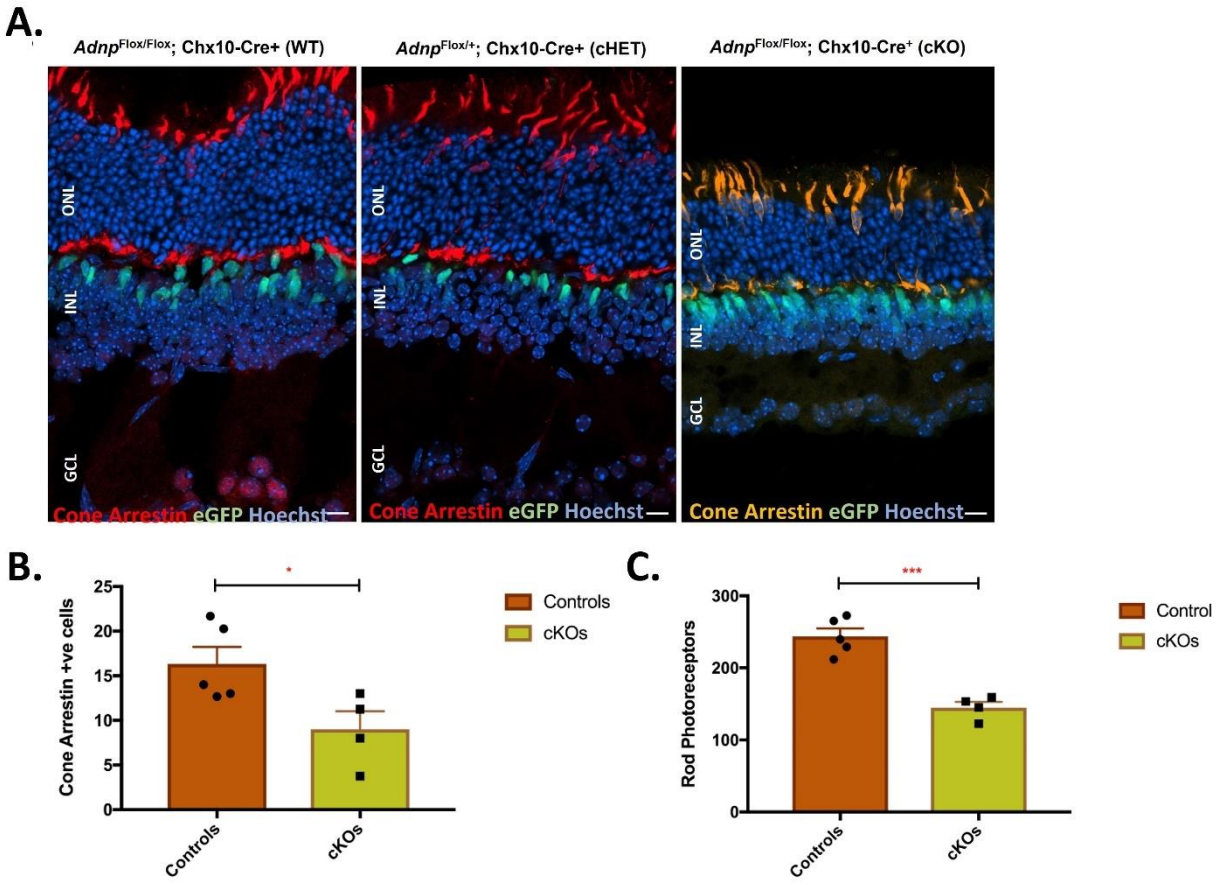

Figure 3.5 Cone and rod cells are significantly reduced in number in cKO retinas

A.) Cone arrestin immunostaining on P21 retinal sections of the WT, cHET and cKO retinas. Cone arrestin specifically labels cones (B). Cone arrestin -negative cells are considered as rod photoreceptors (C). Bar chart comparison of pooled controls vs cKO (absolute counts) for cone (Cone arrestin +) and rod cells (Cone arrestin -negative). Both cell populations were significantly decreased in cKO retina compared to controls (B, C). Statistical analysis was performed using unpaired Student's t-test (P-value for cones = 0.03; P-value for Rods = 0.0003)

3.2.6 Significantly reduced number of bipolar cells in the cKO retina

Otx2 is a homeodomain transcription factor expressed in photoreceptor cells within the ONL, and bipolar cells within the INL of the adult retina[79]. To examine whether Adnp loss impacts upon the bipolar cell population, I performed Otx2 staining on P21 retinas and counted Otx2+ cells in each genotype for analysis. Chx10-Cre GFP also marks both bipolar cells and Müller glial cells in Cre^{+ve} animals. Hence, cells that are GFP+ and Otx2+ were considered for bipolar cell counts. The total

cell counts of bipolar cells were also significantly decreased in cKOs compared to controls (Figure 3.6B).

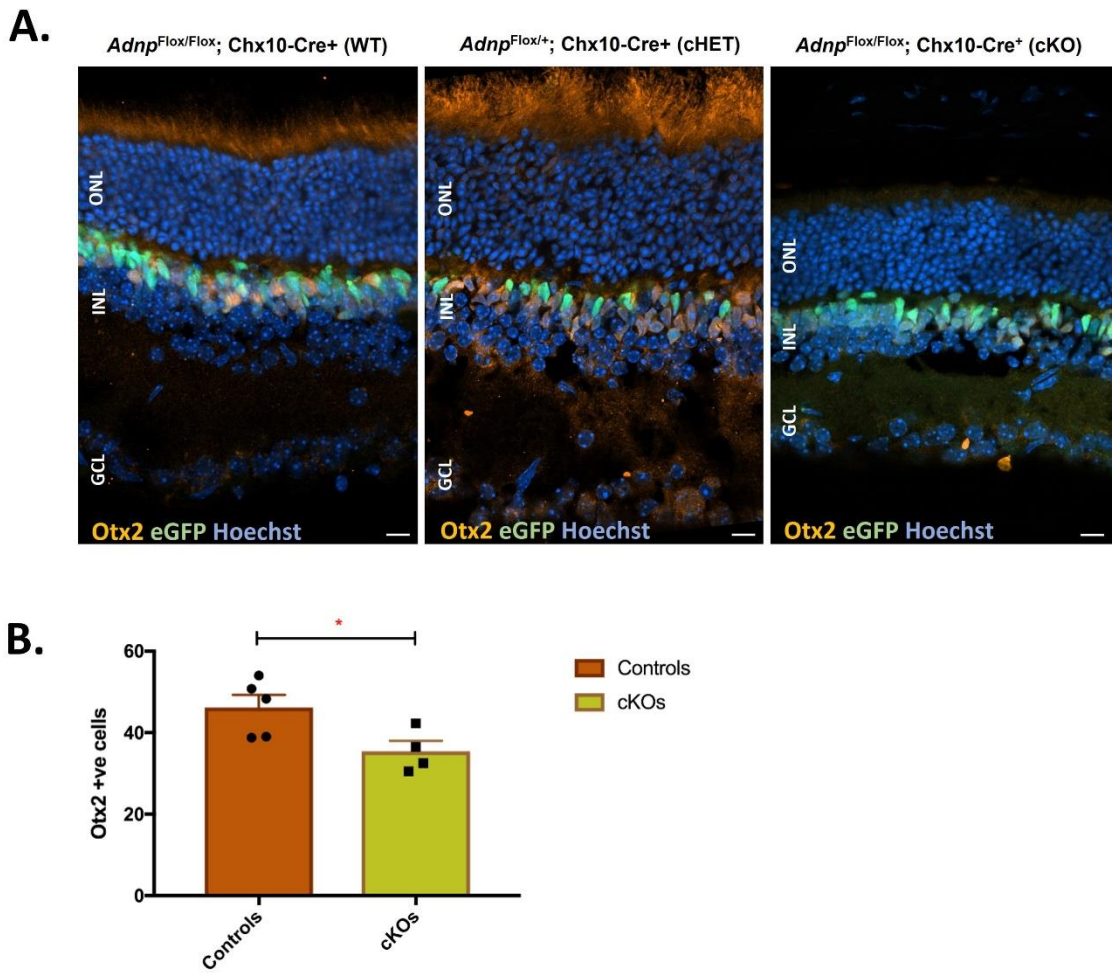

Figure 3.6 Bipolar cells are significantly reduced in cKO retinas

A.) Otx2 immunostaining on P21 retinal sections of the WT, cHET and cKO retinas. Otx2 specifically labels bipolar cells in the INL, and photoreceptors in the ONL. Chx10-GFP also marks the bipolars and Müller glia cells. B.) Bar chart comparison of pooled controls vs cKO (absolute) counts of Otx2+ bipolar cells. Bipolars are significantly decreased in cKO retina compared to controls. Statistical analysis was performed using using the unpaired Student's t-test (P-value = 0.03)

3.2.7 Significantly reduced number of Amacrine cells in cKO retina

In mature retina, Pax6 is expressed in amacrine and ganglion cells[80]. To examine whether Adnp inactivation altered the amacrine cell population, I performed Pax6 immunostaining on retinal cryosections and counted Pax6+ cells in the INL of controls and cKOs (Figure 3.7A). Pax6+ INL cells were also significantly reduced in cKOs (Figure 3.7B).

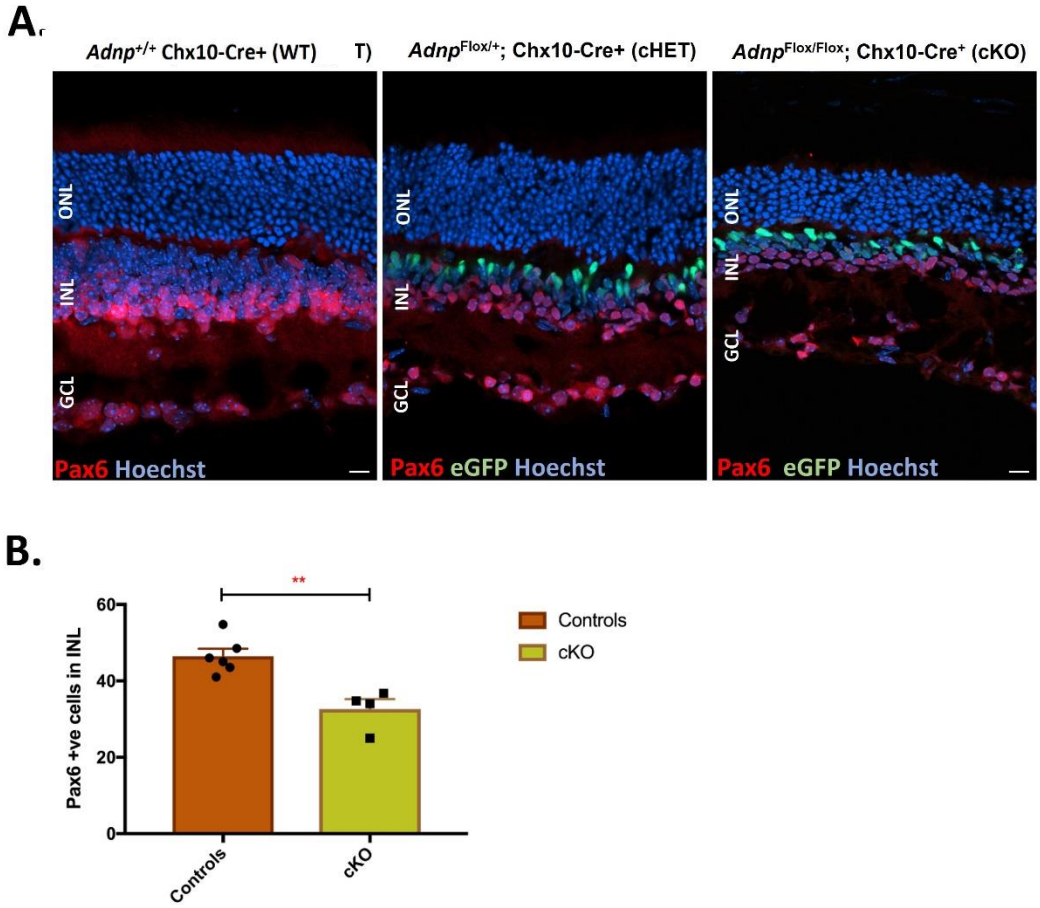

Figure 3.7 Pax6+ amacrine cells are reduced in the INL of cKO retinas

A.) Pax6 immunostaining on P21 sections of the WT, cHET and cKO retinas. Within the INL, Pax6 specifically labels amacrine cells. B.) Comparison of pooled controls vs cKO total counts of pax6 + cells in the INL. Amacrines are significantly decreased in number in the cKO retina compared to controls. Scale bar = 10 μm. Statistical analysis was performed using unpaired Student's t-test (P-value = 0.0025)

3.2.8 Müller glial cells in the cKO retina

In P21 retinas, Sox2 is expressed in Müller glia and cholinergic amacrine cells[81]. The amacrines are clearly distinguishable because of their shape/size and position (basal INL and GCL). However, I also did double staining with Pax6 which is specific to amacrines. For glial cell counts, I counted Sox2+ve cells and ignored cells that were double stained with Pax6 (Figure 3.8A). A decreasing trend was observed but no significant difference was found in the absolute number of Müllers (Figure 3.8B). Moreover, a few Müller glia were observed in the *Adnp* cKOs with mislocalized nuclei in the ONL that are GFP+ and Sox2+ (Figure 3.8A, arrow).

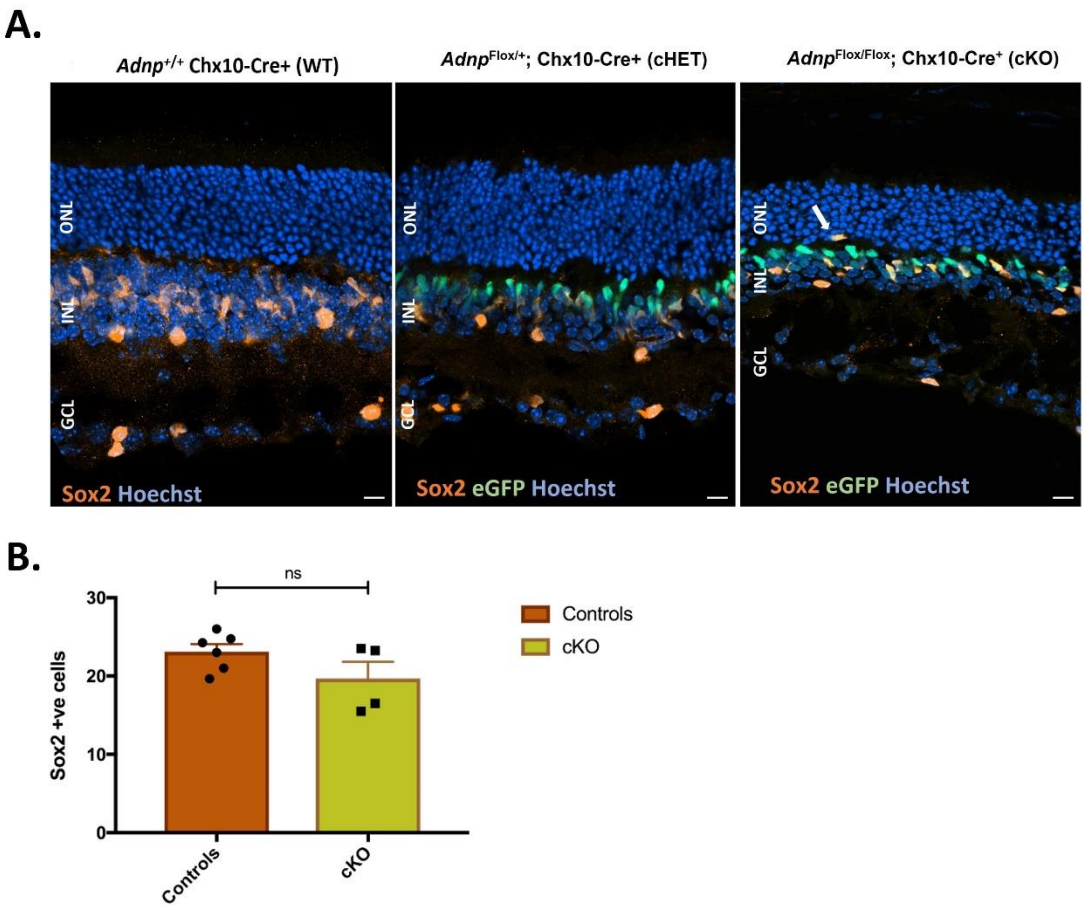

Figure 3.8 Sox2+ Müller glia.

A.) Sox2 immunostaining on P21 retinal sections of the WT, cHET and cKO retinas. Sox2 labels Müller glial cells and a subset of amacrine cells in the P21 retina. The arrow indicates the GFP+ and Sox2 -labelled cells in the ONL of cKO retina. B.) Total counts of Sox2-labelled glial cells for pooled control (WT and cHET) vs cKO. Statistical analysis was performed using unpaired Student's t-test (P-value = 0.1395, ns)

3.2.9 Migration defects in *Adnp* cKOs

Apart from quantitating the cell-type composition of the *Adnp* cKO retina, I additionally examined the organization of cells within the tissue. Using cell-type specific antibodies, I observed mislocalization of Müller glial cells, bipolar and ganglion cells. As mentioned above, I used Sox2 to label the Müller glial cells. In control retina, Sox2+ Müller glial cells were found in the INL, whereas in cKO retinas, some Sox2+ cells were spotted in the ONL (Figure 3.9 A, B). These cells

were oftentimes GFP+, and were negative for Pax6, indicating that they were not amacrine cells. Similarly, Otx2 labelled bipolar cells were found in the INL of control retina, but in cKOs, some Otx2 labelled and GFP+ bipolar cells were also found in the ONL (Figure 3.9 C, D). In the mouse retina, RBPMS is only expressed by ganglion cells[82]. In control retinas, retinal ganglion cells were located in GCL whereas some RBPMS+ cells were also found in the ONL and the INL of cKO retinas (Figure 3.9 E, F). I found that Adnp loss resulted in significant changes to the migration of retinal cells into their appropriate destinations.

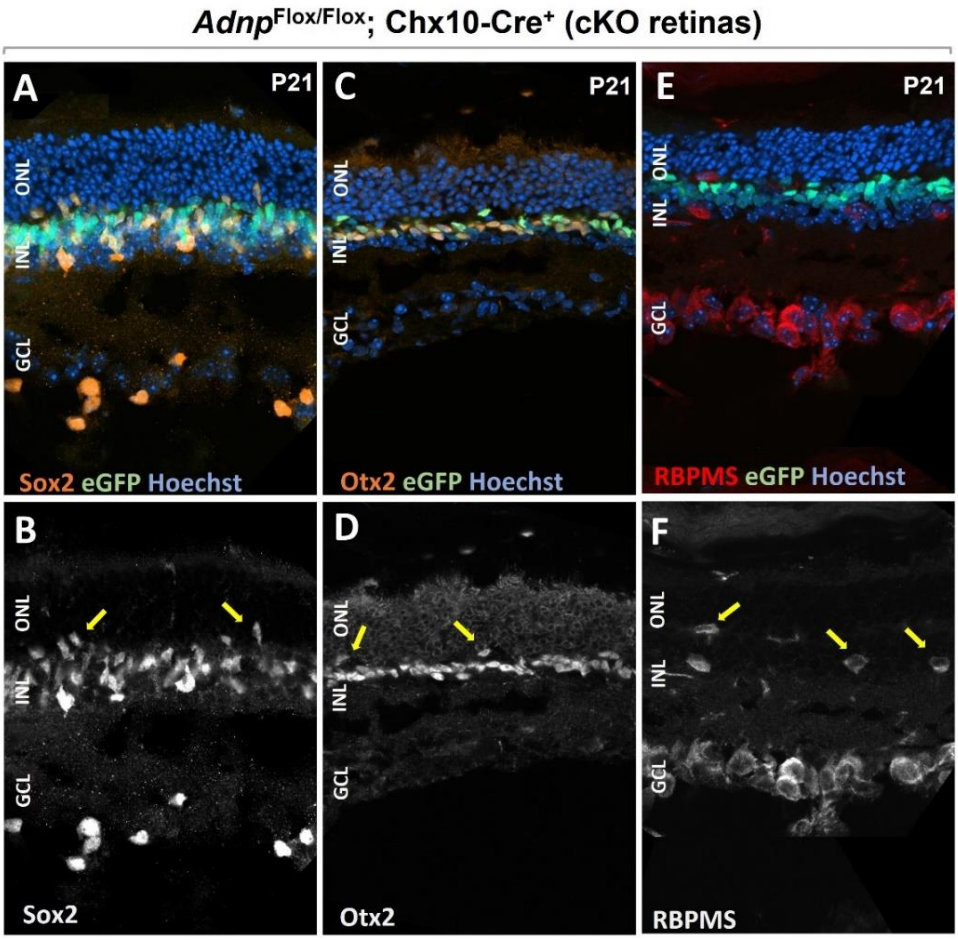

Figure 3.9 Ectopic cells spotted in adult cKO retinas.

Immunostainings on P21 cKO retinal sections- Sox2 staining (Orange) Müller glial cells were found in ONL of cKOs (A). Otx2 labelled and GFP+ bipolar cells were also found in ONL (C). RBPMS specifically labels ganglion cells, which were found in the ONL and INL in cKO retinas. Greyscale image of Sox2+ cells (B), Otx2+ cells (D) and RBPMS+ cells (F). Arrows indicate the displaced Müllers, bipolars and ganglion cells.

3.3 Increased active Caspase3 -positive cells in cKO retinas

Next, to better understand how Adnp regulates retinal size, I examined apoptosis. In preliminary experiments, I immunostained P21 retinal sections with activated Caspase3. I found that there was no apparent increase in the number of apoptotic cells in cKOs compared to controls. We next examined whether Adnp has a role in developmental apoptosis. To assess apoptosis during

development, I immunostained P0 retinal sections to detect activated caspase3. In preliminary experiments, there appeared to be an increase in activated caspase3^{+} cells in P0 cKOs compared to WT retinas (Figure 3.10). I analyzed WT (n=3) and cKO (n=2) retinas. In WT retinas, only neurons were labelled by activated caspase3 – usually located within the GCL, whereas in cKOs, activated caspase3 staining was also observed in proliferating GFP+ cells at the apical surface (Figure 3.10A). These data suggest that Adnp might play a crucial role in cell survival during development.

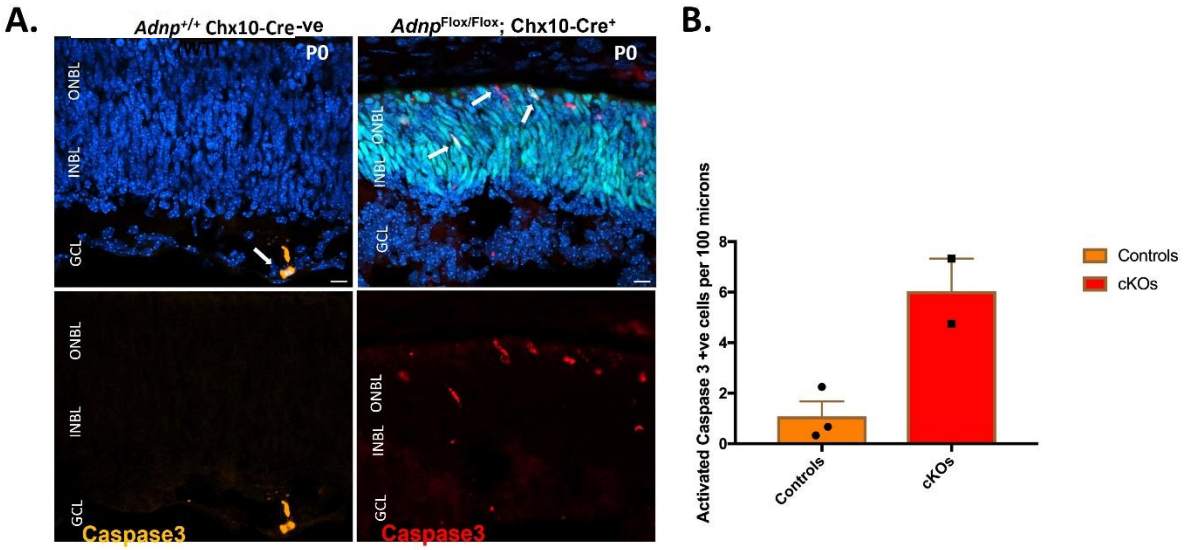

Figure 3.10 Proliferating cells appear to be prone to apoptosis in the Adnp cKO retina

A.) Activated caspase3 immunostaining of P0 WT and cKO retinas. Retinal cryosections were immunostained with anti- activated caspase3 (orange/Red), and the nucleus was counterstained by Hoechst (fluorescent stain; blue). Cre+ve animals express EGFP (Green). ONBL, outer neuroblastic layer; INBL, inner neuroblastic layer; GCL, ganglion cell layer. Bars, 10 μm. In WT, the arrow points to Activated Caspase3 +ve neurons in GCL whereas in cKOs, the arrows are pointed to activated Caspase3 +ve proliferating cell in the ONBL

Chapter 4: IDENTIFICATION OF PUTATIVE ADNP INTERACTING PARTNERS

4.1.1 Adnp interactions with NuRD subunits

To gain insight into the biological pathways that are utilized by Adnp to regulate retinal development, I performed co-immunoprecipitation (co-IP) experiments using mouse retinal tissue. As mentioned above, studies have previously reported that Adnp interacts with proteins such as HP1γ, Chd4, Brg1 and Pogz to regulate neural gene expression during neurogenesis. To examine whether Adnp interacts with these proteins in the retina, I performed co-IP assays to isolate Adnp and its binding partner proteins from mouse retina lysates. I first examined whether Adnp interacted with Chd4 (a prominent subunit of the NuRD complex) during retina development, so I dissected retinas from postnatal developmental stages (P0 and P7). I performed co-IPs with Adnp or Chd4 antibodies and used non-specific IgG as a negative control. Next, I performed western blots, probed with Chd4 antibodies. A faint Chd4 band was observed in Adnp co-IPs (Figure 4.1A). Likewise, when probed with Adnp antibodies, a prominent Adnp band was found in the Chd4 co-IP lane (Figure 4.1B). Antibodies were probed onto the membrane without stripping the membrane in between to avoid loss of proteins. The experiment was repeated three times. Likewise, bands were observed in both Adnp and Chd4 co-IP lanes at respective protein size and not in the IgG IP (Figure 4.1 A, B), confirming that the co-IP antibodies successfully pulled down their respective target proteins. These experiments confirm that Adnp interacts with Chd4 during retinal development.

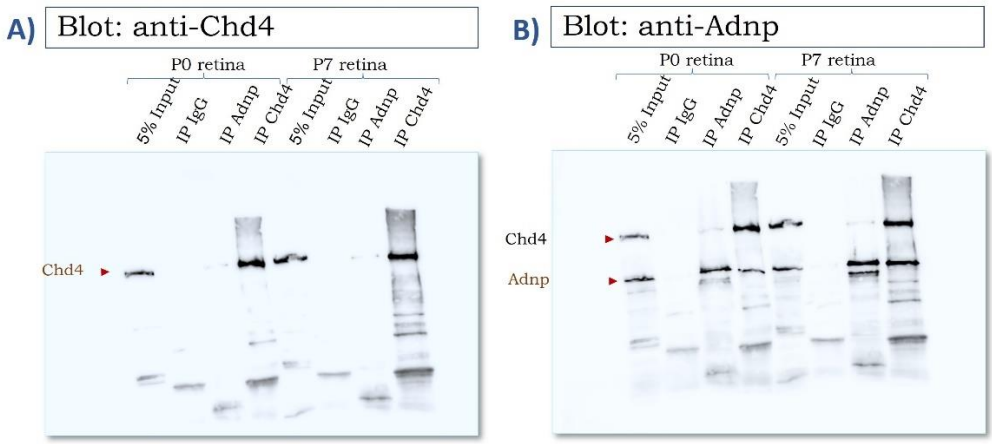

Figure 4.1 Adnp interacts with Chd4 in mouse retina

Total proteins were extracted from P0 and P7 WT retinas and equal amounts were used to set up each co-IP (IgG, Adnp, or Chd4). 5% of the input sample was loaded as positive control and IP IgG served as a negative control. Predicted molecular weights (MW) for Chd4 and Adnp were 226 kDa and 123 kDa, respectively. (A,B) Bands were observed in both IP Adnp, IP Chd4 at approximate sizes after probing with respective antibodies (arrowheads).

4.1.2 Adnp does not interact with Brg1, but binds to Pogz in the mouse retina

Next, I examined whether Adnp interacts with other proteins that were previously reported in the literature. I performed co-IPs on P21 retinas. When the membrane was probed with Chd4, there were prominent bands in IP Chd4, and faint bands were seen in IP Adnp (Figure 4.2A. i). Next, I probed with Brg1. No bands were apparent in IP Adnp (Figure 4.2A. ii). I next probed the membrane with Adnp and a prominent band was evident in both IP chd4 and IP Adnp (Figure 4.2A. iii). These results suggests that the Adnp and Chd4 IP's worked and yet Adnp did not pull down Brg1, further confirming that Adnp interacts with Chd4 but not with Brg1 in the mouse retina. To investigate whether Adnp interacts with Pogz, I also performed westerns using a Pogz antibody. I observed a prominent band in IP Adnp and Chd4 when the membrane was probed with Pogz (Figure 4.2B. i).

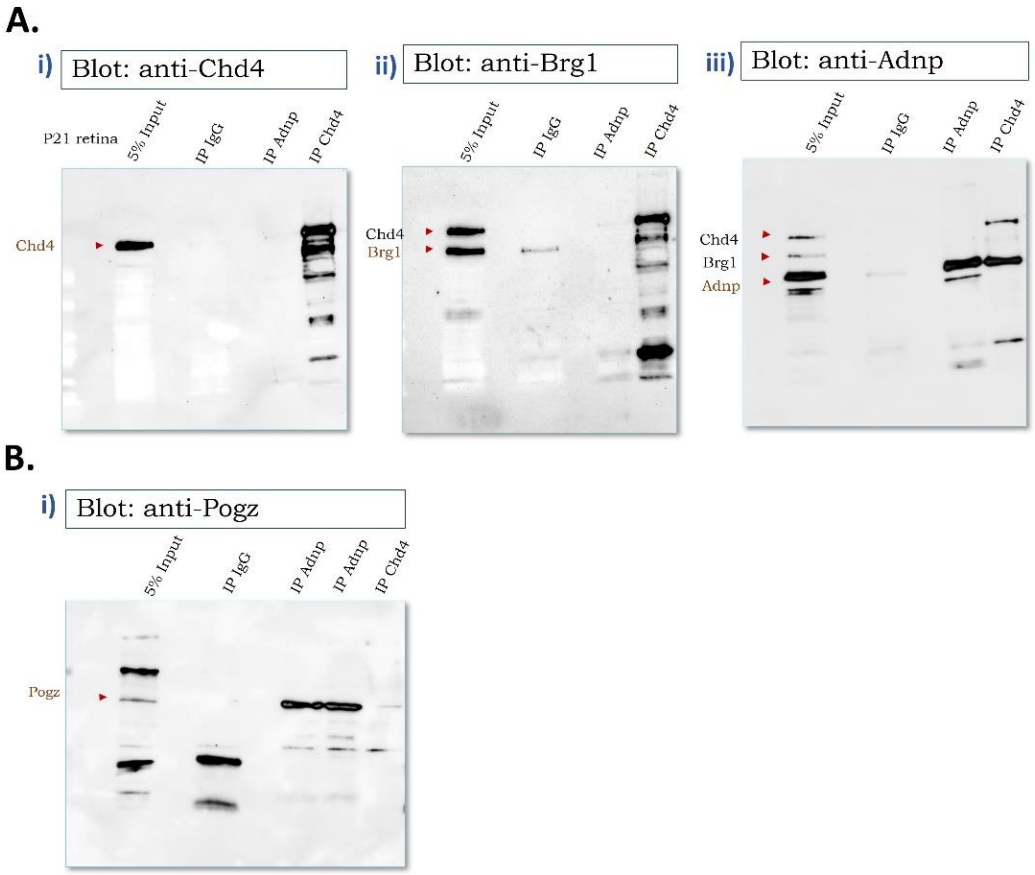

Figure 4.2 Adnp interacts Pogz but not with Brg1 in mouse retina

A. i) Membrane probed with Chd4 and a faint band was observed in IP Adnp. A strong band was observed in IP Chd4 as expected. B.ii) The membrane was probed for Brg1 and no bands were found for IP Adnp. MW of Brg1 is 184 kDa. B. iii) The membrane was probed with Adnp and a prominent band was observed in IP Chd4 as expected. B. i) The membrane was probed with Pogz and prominent bands were found in the IP Adnp lanes. MW of Pogz is 155 kDa.

4.1.3 Inactivation of Adnp alters Pogz expression

I next examined whether Pogz protein levels might be altered in cKO retinas, since the converse effect was observed in *Pogz* KO brains[60]. I performed western blot on P0 retinas from three genotypes. Interestingly Pogz seemed decreased in cKO compared to WT and cHET samples (Figure 4.3A). I performed densitometry to compare protein abundance between samples after normalizing against beta-actin and observed that Pogz levels were significantly decreased in the

cKO retina (Figure 4.3B). This data suggests that inactivation of Adnp could alter the expression of Pogz in the retina.

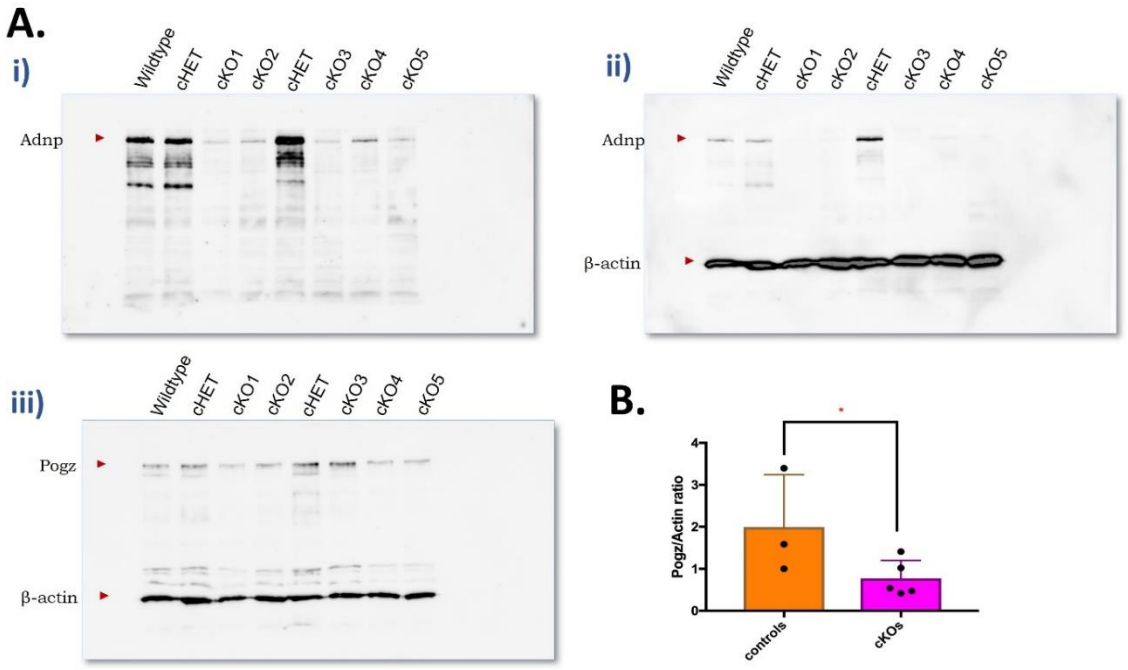

Figure 4.3 Significant decrease in Pogz levels in cKO retinas

Proteins were extracted from P0 retinas of the WT, cHET and cKO animals. Proteins were separated by SDS-PAGE. (A. i) Western blot showing Adnp expression. (A. ii) Western blot showing β-actin expression. (A. iii) Pogz was probed on the same membrane. Pogz levels seemed to be reduced in cKO lanes. (B) Pogz expression was normalized against β-actin. Graph represents the Pogz/Actin ratios calculated based on protein abundance comparing pooled controls (WT, cHET) and cKO samples. Statistical analysis was performed using Unpaired t test (P-value = 0.003)

CHAPTER 5: DISCUSSSION

5.1 Adnp expression was consistent during retina development

To investigate the role of Adnp in retinal development, we first investigated Adnp protein expression at different developmental stages. In mouse, retina development occurs between embryonic day E11 and post-natal day P11. We found that Adnp was consistently expressed throughout retinal development. Adnp was expressed in all retinal progenitor cells. Interestingly differentiated cells were found to have increased expression of Adnp. Moreover, protein expression was maintained in all cell types in an adult/P21 retina. From the Adnp expression profile, it appears that different types of neurons and glia express Adnp to varying degrees. RGCs seem to express Adnp very highly, whereas expression levels are quite low in rods. It is evident that Adnp might have multiple roles in retinal development.

5.2 Generation of a retina specific *Adnp* knockout mouse model

Germline *Adnp* knockout is lethal. Over the past two decades, studies were performed to understand Adnp's functions based on its interactions with other proteins, its localization on chromatin and by identifying target genes – primarily using a variety of cell lines. Other studies were focused on understanding ADNP pathophysiology by analyzing mouse models that mimic HVDAS conditions (ie. haploinsufficiency). However, not much is known about Adnp's *in vivo* role. The goal of my project was thus to generate an appropriate model to study Adnp's functions in neurogenesis. Therefore, we generated an *Adnp* floxed allele using the CRISPR/Cas9 system. Then, the floxed mice were crossed with *Chx10-Cre* transgenic mice to conditionally knockout Adnp specifically in the developing retina. Our data demonstrate that the Cre-loxP recombination system has been an efficient tool for targeted Adnp inactivation in retina. Initially, we faced issues

with Cre mosaicism associated with *Chx10-Cre* transgenic mice (Figure 2.3). However, we were able to develop measures that permitted mosaicism to be managed. Transgenes are often integrated into the chromosome as a multicopy concatemer[83]. These concatemers sometimes spontaneously rearrange – oftentimes via recombination events. Hence it is crucial to characterize the transgene by examining the copy number. Quantitative PCR is one of the best methods to identify the copy number variation with appropriate primers designed for the integration site. In this study we used *Chx10-Cre* primers to estimate the copy number of Cre as mentioned in the Material and Methods section (Figure 2.3). Based on relative band intensity, which is approximately proportional to the amount of integrated copy number, we were able to distinguish between normal and mosaic *Chx10-Cre* alleles. In order to limit Cre mosaicism, testing animals for genotypes and carefully selecting parent animals was very important.

5.3 Adnp loss causes retinal hypoplasia

A previous study reported that inactivation of *Adnp* in mouse ESCs led to the formation of smaller embryonic bodies[43]. Similarly, in the *Adnp*-cKO retinas, I found that loss of Adnp resulted in formation of smaller retinas. Not much is known about Adnp's role in the growth of neural progenitor cells due to lack of appropriate models. Now, we have established a good model to understand how exactly Adnp regulates neural development. Further, I have shown that *Adnp*-cKO retinas have a significantly reduced number of almost all retinal cell types. In preliminary experiments, I have also performed analysis for horizontal and ganglion cells, and these seem to be decreased in cKO retinas. From this data, it is evident that Adnp is crucial for proper retinal development. Moreover, we found some ectopic cells in cKO retinas. These results suggest that the loss of Adnp also caused impairments in cell migration during retinal development.

5.4 Increased apoptosis in P0 cKO retina

From the P21 cell count data, we hypothesized that Adnp might either be essential for RPC survival or might control the multistep process of RPC proliferation. Using an activated Caspase3 antibody, I have also found evidence that suggests that part of the phenotype might be due to increased apoptosis during development. However, these findings were also consistent with previous studies reporting increased cell death in *Adnp* knockout ES cells.[43] We still do not know when cells are dying, and whether the elevated cell death that is indicated by immunohistochemistry fully accounts for the decrease in overall retinal size and cell number. Activated Caspase3 staining needs to be done at several stages in order to better understand whether Adnp is truly associated with cell death. In preliminary experiments, I have also examined cell proliferation in P0 retinas using Ki67 and Phospho-histone H3 (pHH3) antibodies, and future work should use this approach to determine whether altered proliferation might also play a role in the hypoplasia observed in Adnp cKOs.

As mentioned in the Introduction, an ophthalmic study on an HVDAS child identified structural defects in the retina and delayed maturation of the visual system. The study suggested that mutation in the *ADNP* gene may cause dysgenesis of the retina in HVDAS patients. Although the *Adnp*-cKO model does not mimic the genetics of HVDAS, our findings suggest that Adnp plays a vital role in proper development of retina. Hence, an early eye examination might be helpful for HVDAS patients to address potential eye conditions and treatments.

5.5 Adnp interacts with Chd4 and not with Brg1 in mouse retina

The second objective of my project was to identify Adnp binding partners in mouse retina, in order to permit better understanding of the biological mechanisms through which Adnp regulates

neurodevelopment. As mentioned in the Introduction, previous studies have identified Adnp-interacting proteins, and some showed that Adnp interacts with Brg1 and other subunits of SWI/SNF chromatin remodelling complex[58]. Other studies showed that Adnp interacts with Chd4[43,59]. In our CoIP experiment results, we did not observe interactions between Adnp and Brg1. In addition, we haven't found Brg1 in unbiased proteomic screens (unpublished). Moreover, the phenotypes observed in *Adnp*-cKO and *Brg1*-cKO retinas were very different. Brg1 was required to regulate retinal lamination and the cKO retina has extensive disorganization of retinal layers and defects in RPC polarity[84]. Whereas in *Adnp*-cKOs, no defects in retinal lamination were observed. Moreover, persistent proliferating cells were identified in P21 *Brg1*-deficient retinas, whereas no proliferative/Ki67+ cells were found in P21 *Adnp*-cKO retina (data not shown).

Our data demonstrate that Adnp strongly interacts with Chd4 in the mouse retina. Our data suggest that Adnp binds with Chd4, and that Adnp might regulate gene expression during development via chromatin remodelling. Moreover, Sujay Shah, a PhD candidate in our lab evaluated the *Chd4*-cKO model using the same Chx10-Cre mice (unpublished). Interestingly *Adnp*-cKO and *Chd4*-cKO P21 retinas seem very similar and in both there were reduced number of ONL and INL cells. There are also mislocalized glial cells in both models.

We identified Pogz as another interacting partner of Adnp in the retina. It has been shown that heterozygous Pogz animals have reduced Adnp expression levels in the brain[60]. We also found that Pogz protein levels were reduced in *Adnp* cKO retinas. Further experiments could help in understanding how risk genes associated with neurodevelopmental disorders function together to regulate gene expression.

5.6 Future prospectives

Overall, an in-depth characterization of the *Adnp*-cKO model remains to be completed. Indeed, although I have observed morphological changes in adult/ P21 retinas using cell type markers, and increased apoptosis in P0 retinas, the phenotype may be influenced by a variety of factors. In order to elucidate the phenotype origin, proliferation and survival of retinal progenitor cells must be assessed. Performing birthdating experiments will reveal whether Adnp has a role in developmental delays. Ectopically mislocalized cells could result from neurons and glia being born outside of their normal developmental windows. Further co-IP's followed by mass spectrometry (MS) analysis would provide the list of Adnp binding partners that could allow us to define the Adnp functional complexes and determine the precise mechanisms by which they regulate retinal neurogenesis. Lastly, to understand how Adnp influences gene expression and development in neural cells in the retina, CUT&RUN and scRNA-seq needs to be performed. These experiments will allow us to identify genes that are direct targets of Adnp and to determine how Adnp affects transcription (as an activator or repressor) on differently regulated genes.

Supplementary figures

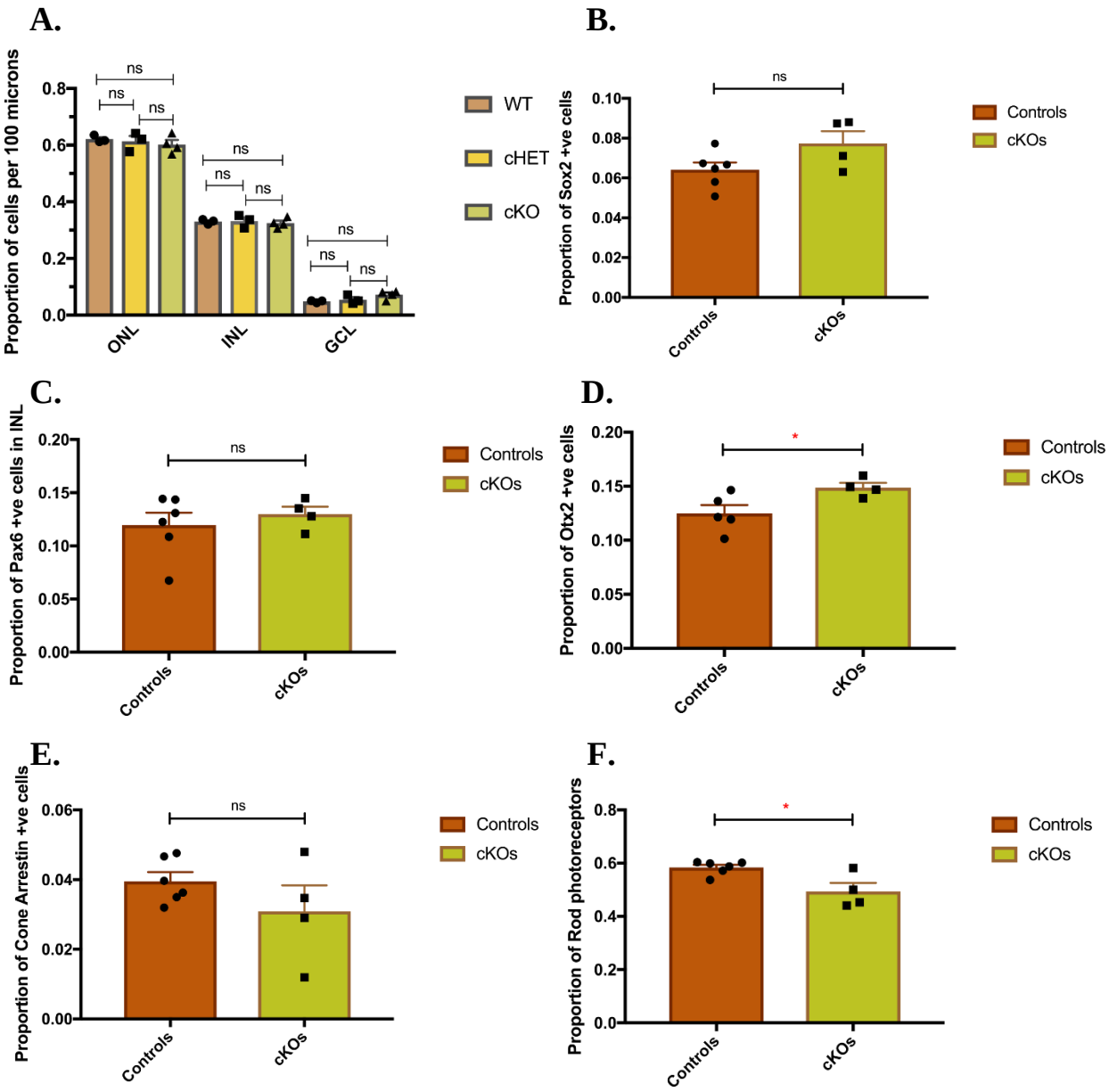

Supplementary Figure 1: Corresponding proportional analysis on cell counts of controls and cKO retinas.

A.) Proportional analysis showed no statistically significant difference between retinal layers in WT, cHET and cKO groups. (B-F) Comparison of pooled control vs cKO proportional analysis of Sox2+, Pax6+, Otx2+, Cone arrestin +, Cone arrestin- labelled mullers, amacrines, bipolar, cone and rod cells. It is evident from the total cell count analysis that rod cells are dramatically reduced in cKOs. This effect leads to corresponding increase in proportions of other cell types in proportional analysis.

REFERENCES

1. Pearson, B. J. & Doe, C. Q. Specification of temporal identity in the developing nervous system. *Annual Review of Cell and Developmental Biology* vol. 20 619–647 Preprint at https://doi.org/10.1146/annurev.cellbio.19.111301.115142 (2004).

2. Adler, R. & Valeria Canto-Soler, M. *Molecular mechanisms of optic vesicle development: Complexities, ambiguities and controversies*.

3. Schmitt, E. A. & Dbwling, J. E. *Early Eye Morphogenesis in the Zebrafish, Brachydanio rerio*. *THE JOURNAL OF COMPARATIVE NEUROLOGY* vol. 344 (1994).

4. Fuhrmann, S. *Eye morphogenesis and patterning of the optic vesicle*. *Current Topics in Developmental Biology* vol. 93 (2010).

5. Zuber, M. E., Gestri, G., Viczian, A. S., Barsacchi, G. & Harris, W. A. Specification of the vertebrate eye by a network of eye field transcription factors. *Development* **130**, 5155–5167 (2003).

6. Hsieh, Y. W. & Yang, X. J. Dynamic Pax6 expression during the neurogenic cell cycle influences proliferation and cell fate choices of retinal progenitors. *Neural Dev* **4**, (2009).

7. FitzPatrick, D. R. & Van Heyningen, V. Developmental eye disorders. *Current Opinion in Genetics and Development* vol. 15 348–353 Preprint at https://doi.org/10.1016/j.gde.2005.04.013 (2005).

8. Loosli, F. *et al.* Loss of eyes in zebrafish caused by mutation of chokh/rx 3. *EMBO Rep* **4**, 894–899 (2003).

9. Stenkamp, D. L. Development of the Vertebrate Eye and Retina. in *Progress in Molecular Biology and Translational Science* vol. 134 397–414 (Elsevier B.V., 2015).

10. Snyder, E. Y. *Lineage-Independent Determination of Cell Type in the Embryonic Mouse Retina*. *Neuron* vol. 4 (1990).

11. Young, R. W. *Cell Differentiation in the Retina of the Mouse*. *THE ANATOMICAL RECORD* vol. 212 (1985).

12. la Vail, M. M. & Rapaport, D. H. *Cytogenesis in the Monkey Retina*. *THE JOURNAL OF COMPARATIVE NEUROLOGY* vol. 309 (1991).

13. Rapaport, D. H., Wong, L. L., Wood, E. D., Yasumura, D. & Lavail, M. M. Timing and topography of cell genesis in the rat retina. *Journal of Comparative Neurology* **474**, 304–324 (2004).

14. Wong, L. L. & Rapaport, D. H. Defining retinal progenitor cell competence in Xenopus laevis by clonal analysis. *Development* **136**, 1707–1715 (2009).

15. Belecky-Adams, T., Cook, B. & Adler, R. *Correlations between Terminal Mitosis and Differentiated Fate of Retinal Precursor Cells in Vivo and in Vitro: Analysis with the ‘‘‘Window-Labeling’’’ Technique*. *DEVELOPMENTAL BIOLOGY* vol. 178 (1996).

16. Marquardt, T. & Gruss, P. Generating neuronal diversity in the retina: one for nearly all. *Trends Neurosci* **25**, 32–38 (2002).

17. Livesey, F. J. & Cepko, C. L. Vertebrate neural cell-fate determination: Lessons from the retina. *Nat Rev Neurosci* **2**, 109–118 (2001).

18. Cepko, C. L. The roles of intrinsic and extrinsic cues and bHLH genes in the determination of retinal cell fates. *Curr Opin Neurobiol* **9**, 37–46 (1999).

19. turner1987.

20. Wetts, R. & Fraser, S. E. Multipotent Precursors Can Give Rise to All Major Cell Types of the Frog Retina. *Science (1979)* **239**, 1142–1145 (1988).

21. Cepko, C. L., Austin, C. P., Yang, X., Alexiades, M. & Ezzeddine, D. *Cell fate determination in the vertebrate retina*. vol. 93 (1996).

22. He, J. *et al.* How Variable Clones Build an Invariant Retina. *Neuron* **75**, 786–798 (2012).

23. Gomes, F. L. A. F. *et al.* Reconstruction of rat retinal progenitor cell lineages in vitro reveals a surprising degree of stochasticity in cell fate decisions. *Development* **138**, 227–235 (2011).

24. Wong, L. L. & Rapaport, D. H. Defining retinal progenitor cell competence in *Xenopus laevis* by clonal analysis. *Development* **136**, 1707–1715 (2009).

25. Bassett, E. A. & Wallace, V. A. Cell fate determination in the vertebrate retina. *Trends in Neurosciences* vol. 35 565–573 Preprint at https://doi.org/10.1016/j.tins.2012.05.004 (2012).

26. Buono, L. & Martinez-Morales, J. R. Retina Development in Vertebrates: Systems Biology Approaches to Understanding Genetic Programs: On the Contribution of Next-Generation Sequencing Methods to the Characterization of the Regulatory Networks Controlling Vertebrate Eye Development. *BioEssays* vol. 42 Preprint at https://doi.org/10.1002/bies.201900187 (2020).

27. Ohsawa, R. & Kageyama, R. Regulation of retinal cell fate specification by multiple transcription factors. *Brain Research* vol. 1192 90–98 Preprint at https://doi.org/10.1016/j.brainres.2007.04.014 (2008).

28. Marquardt, T. *et al.* Pax6 Is Required for the Multipotent State of Retinal Progenitor Cells. *Cell* **105**, 43–55 (2001).

29. Vitorino, M. *et al.* Vsx2 in the zebrafish retina: restricted lineages through derepression. *Neural Dev* **4**, 14 (2009).

30. Matsushima, D., Heavner, W. & Pevny, L. H. Combinatorial regulation of optic cup progenitor cell fate by SOX2 and PAX6. *Development* **138**, 443–454 (2011).

31. Mears, A. J. *et al.* Nrl is required for rod photoreceptor development. *Nat Genet* **29**, 447–452 (2001).

32. Liu, W., Mo, Z. & Xiang, M. The *Ath5* proneural genes function upstream of *Brn3* POU domain transcription factor genes to promote retinal ganglion cell development. *Proceedings of the National Academy of Sciences* **98**, 1649–1654 (2001).

33. Neumann, C. J. & Nuesslein-Volhard, C. Patterning of the Zebrafish Retina by a Wave of Sonic Hedgehog Activity. *Science (1979)* **289**, 2137–2139 (2000).

34. Bernardos, R. L., Lentz, S. I., Wolfe, M. S. & Raymond, P. A. Notch–Delta signaling is required for spatial patterning and Müller glia differentiation in the zebrafish retina. *Dev Biol* **278**, 381–395 (2005).

35. Martinez-Morales, J. R. *et al.* Differentiation of the vertebrate retina is coordinated by an FGF signaling center. *Dev Cell* **8**, 565–574 (2005).

36. Meyers, J. R. *et al.* β-catenin/Wnt signaling controls progenitor fate in the developing and regenerating zebrafish retina. *Neural Dev* **7**, 30 (2012).

37. Stevens, C. B., Cameron, D. A. & Stenkamp, D. L. Plasticity of photoreceptor-generating retinal progenitors revealed by prolonged retinoic acid exposure. *BMC Dev Biol* **11**, 51 (2011).

38. Seritrakul, P. & Gross, J. M. Genetic and epigenetic control of retinal development in zebrafish. *Current Opinion in Neurobiology* vol. 59 120–127 Preprint at https://doi.org/10.1016/j.conb.2019.05.008 (2019).

39. Khorasanizadeh, S. *Review The Nucleosome: From Genomic Organization to Genomic Regulation*. *Cell* vol. 116 (2004).

40. Millard, C. J. *et al.* The structure of the core NuRD repression complex provides insights into its interaction with chromatin. *Elife* **5**, (2016).

41. Hu, G. & Wade, P. A. NuRD and Pluripotency: A Complex Balancing Act. *Cell Stem Cell* **10**, 497–503 (2012).

42. Mattar, P. *et al.* A Casz1–NuRD complex regulates temporal identity transitions in neural progenitors. *Sci Rep* **11**, (2021).

43. Ostapcuk, V. *et al.* Activity-dependent neuroprotective protein recruits HP1 and CHD4 to control lineage-specifying genes. *Nature* **557**, 739–743 (2018).

44. Pinhasov, A. *et al.* Activity-dependent neuroprotective protein: A novel gene essential for brain formation. *Developmental Brain Research* **144**, 83–90 (2003).

45. Bassan, M. *et al.* Complete sequence of a novel protein containing a femtomolar-activity-dependent neuroprotective peptide. *J Neurochem* **72**, 1283–1293 (1999).

46. Gozes, I. *et al.* NAP: Research and development of a peptide derived from activity-dependent neuroprotective protein (ADNP). *CNS Drug Rev* **11**, 353–368 (2005).

47. Zemlyak, I., Furman, S., Brenneman, D. E. & Gozes, I. *A Novel peptide prevents death in enriched neuronal cultures*. *Regulatory Peptides* vol. 96 www.elsevier.com/locate/regpep (2000).

48. Hacohen-Kleiman, G. *et al.* Activity-dependent neuroprotective protein deficiency models synaptic and developmental phenotypes of autism-like syndrome. *Journal of Clinical Investigation* **128**, 4956–4969 (2018).

49. Gozes, I. Microtubules, schizophrenia and cognitive behavior: Preclinical development of davunetide (NAP) as a peptide-drug candidate. *Peptides* vol. 32 428–431 Preprint at https://doi.org/10.1016/j.peptides.2010.10.030 (2011).

50. Zamostiano, R. *et al.* Cloning and characterazation of the human activity-dependent neuroprotective protein. *Journal of Biological Chemistry* **276**, 708–714 (2001).

51. Gozes, I. *et al.* The eight and a half year journey of undiagnosed AD: Gene sequencing and funding of advanced genetic testing has led to hope and new beginnings. *Front Endocrinol (Lausanne)* **8**, (2017).

52. Larsen, E. *et al.* A systematic variant annotation approach for ranking genes associated with autism spectrum disorders. *Mol Autism* **7**, (2016).

53. Satterstrom, F. K. *et al.* Large-Scale Exome Sequencing Study Implicates Both Developmental and Functional Changes in the Neurobiology of Autism. *Cell* **180**, 568-584.e23 (2020).

54. van Dijck, A. *et al.* Clinical Presentation of a Complex Neurodevelopmental Disorder Caused by Mutations in ADNP. *Biol Psychiatry* **85**, 287–297 (2019).

55. Helsmoortel, C. *et al.* A SWI/SNF-related autism syndrome caused by de novo mutations in ADNP. *Nat Genet* **46**, 380–384 (2014).

56. Thiru, A. *et al.* Structural basis of HP1/PXVXL motif peptide interactions and HP1 localisation to heterochromatin. *EMBO J* **23**, 489–499 (2004).

57. Mandel, S., Rechavi, G. & Gozes, I. Activity-dependent neuroprotective protein (ADNP) differentially interacts with chromatin to regulate genes essential for embryogenesis. *Dev Biol* **303**, 814–824 (2007).

58. Mandel, S. & Gozes, I. Activity-dependent neuroprotective protein constitutes a novel element in the SWI/SNF chromatin remodeling complex. *Journal of Biological Chemistry* **282**, 34448–34456 (2007).

59. Tabar, M. S., Giardina, C., Feng, Y. J. & Francis, H. Unique Protein Interaction Networks Define The Chromatin Remodeling Module of The NuRD Complex. (2021).

60. Markenscoff-Papadimitriou, E. *et al.* Autism risk gene POGZ promotes chromatin accessibility and expression of clustered synaptic genes. *bioRxiv* 2021.04.07.438852 (2021).

61. Connaughton, D. M. *et al.* Mutations of the Transcriptional Corepressor ZMYM2 Cause Syndromic Urinary Tract Malformations. *The American Journal of Human Genetics* **107**, 727–742 (2020).

62. Sollis, E. *et al.* Characterization of the TBR1 interactome: variants associated with neurodevelopmental disorders disrupt novel protein interactions. *Hum Mol Genet* (2022) doi:10.1093/hmg/ddac311.

63. Kaaij, L. J. T., Mohn, F., van der Weide, R. H., de Wit, E. & Bühler, M. The ChAHP Complex Counteracts Chromatin Looping at CTCF Sites that Emerged from SINE Expansions in Mouse. *Cell* **178**, 1437-1451.e14 (2019).

64. Yan, Q. *et al.* Proximity labeling identifies a repertoire of site-specific R-loop modulators. *Nat Commun* **13**, (2022).

65. Gale, M. J. *et al.* Longitudinal ophthalmic findings in a child with Helsmoortel-Van der Aa Syndrome. *Am J Ophthalmol Case Rep* **10**, 244–248 (2018).

66. Nagy, A. *Cre Recombinase: The Universal Reagent for Genome Tailoring*. (2000).

67. Sauer, B. & Henderson, N. *Site-specific DNA recombination in mammalian cells by the Cre recombinase of bacteriophage P1 (genome rearrangement/herpesviruses/Cre-lox/metalothionein)*. *Proc. Nail. Acad. Sci. USA* vol. 85 (1988).

68. Sternberg, K. & Asd, ? *Bacteriophage Pl Site-specific Recombination I. Recombination Between loxP Sites*. *I. Mol. Riol* vol. 150 (1981).

69. Sternberg, N., Sauer, B., Hoessf, R. & Abremski, K. *Bacteriophage Pl Ere Gene and its Regulatory Region Evidence for Multiple Promoters and for Regulation by DNA Methylation*. *J. Mol. Biol* vol. 187 (1986).

70. O'neil, K. T., Shuman, J. & Degrado, W. F. *Design of DNA-Binding Peptides Based on the Leucine Zipper Motif*. *Biochitn. Biophys. Acta* vol. 44 www.sciencemag.org (1960).

71. Branda, C. S. & Dymecki, S. M. *Review Talking about a Revolution: The Impact of Site-Specific Recombinases on Genetic Analyses in Mice SSRs, Their Target Sites, and Their Function The SSRs Cre (causes recombination of the bacterio-phage P1 genome) and Flp (named for its ability to invert, or 'flip,' a DNA segment in S. cerevisiae) are able to recombine specific sequences of DNA with high fidelity*. *Developmental Cell* vol. 6 http://www. (2004).

72. Giraldo, P. & Montoliu, L. *Size matters: use of YACs, BACs and PACs in transgenic animals*. *Transgenic Research* vol. 10 (2001).

73. Hébert, J. M. & McConnell, S. K. Targeting of cre to the Foxg1 (BF-1) Locus Mediates loxP Recombination in the Telencephalon and Other Developing Head Structures. *Dev Biol* **222**, 296–306 (2000).

74. Marquardt, T. *et al.* Pax6 Is Required for the Multipotent State of Retinal Progenitor Cells. *Cell* **105**, 43–55 (2001).

75. Correction: Rax-CreERT2 Knock-In Mice: A Tool for Selective and Conditional Gene Deletion in Progenitor Cells and Radial Glia of the Retina and Hypothalamus. *PLoS One* **9**, e102875 (2014).

76. Rowan, S. & Cepko, C. L. Genetic analysis of the homeodomain transcription factor Chx10 in the retina using a novel multifunctional BAC transgenic mouse reporter. *Dev Biol* **271**, 388–402 (2004).

77. Liu, I. S. C. *et al. Developmental Expression of a Novel Murine Homeobox Gene (C/1x10): Evidence for Roles in Determination of the Neuroretina and Inner Nuclear layer*. *Neuron* vol. 13 (1994).

78. Craft, C. M., Whitmore, D. H. & Wiechmann, A. F. Cone arrestin identified by targeting expression of a functional family. *Journal of Biological Chemistry* **269**, 4613–4619 (1994).

79. Koike, C. *et al.* Functional Roles of Otx2 Transcription Factor in Postnatal Mouse Retinal Development. *Mol Cell Biol* **27**, 8318–8329 (2007).

80. Hitchcock,', P. F., Macdonald, R. E., Vanderyt, J. T., Wilson' ', S. W. & Kellogg, W. K. *Antibodies against Pax6 lmmunostain Amacrine and Ganglion Cells and Neuronal Progenitors, but not Rod Precursors, in the Normal and Regenerating Retina of the Goldfish*.

81. Lin, Y., Ouchi, Y., Satoh, S. & Watanabe, S. Sox2 Plays a Role in the Induction of Amacrine and Müller Glial Cells in Mouse Retinal Progenitor Cells. *Investigative Opthalmology & Visual Science* **50**, 68 (2009).

82. Kwong, J. M. K., Caprioli, J. & Piri, N. RNA Binding Protein with Multiple Splicing: A New Marker for Retinal Ganglion Cells. *Investigative Opthalmology & Visual Science* **51**, 1052 (2010).

83. Bishop, J. O. & Smith, P. Mechanism of chromosomal integration of microinjected DNA. *Mol Biol Med* **6**, 283–98 (1989).

84. Aldiri, I. *et al.* Brg1 coordinates multiple processes during retinogenesis and is a tumor suppressor in retinoblastoma. *Development (Cambridge)* **142**, 4092–4106 (2015).